The Significance of Alternative Energy
Towards Eco-Mobility Era
1st International Conference on Mechanical Engineering - ICOME 2013
September 12-14th, Lombok Island, Mataram, Indonesia
Room D202, Teknik Mesin-FTI-ITS, Kampus ITS, Keputih, Sukolilo, Surabaya, INDONESIA, 60111
Telp.+62-31-5981731, 5938773, Fax. +62-31-5946230, 59338773
Email: icome@its.ac.id, website: http://icome.its.ac.id

Letter of Acceptance and Invitation Letter

Dear Ekadewi Handoyo

On behalf of ICOME 2013 committee, we are pleased to inform you that your paper with the following information,

Paper id	: 69
Title	: Experimental Studies on a Solar Air Heater Having V-Corrugated Absorber Plate with Obstacles Bent Vertically
Organization	: Petra Christian University
Contact author	: ekadewi@peter.petra.ac.id

has been accepted for oral presentation in ICOME 2013. Your paper will be published in **Applied Mechanics and Materials (AMM) Journal** which will be indexed in the major academic databases, including *Elsevier, SCOPUS, Ei Compendex, CSA, CA and ISI (ISTP, CPCI, Web of Science).*

Please note the following:

- Please make the necessary revisions, if any, before submitting the final paper. Kindly send your final paper and the copyright through https://www.easychair.org no later than July 31, 2013.
- The camera-ready version should strictly follow the paper format.
- Presentation will be held on September 12-13, 2013. Detailed schedule will be posted on ICOME website as soon as it becomes available.
- Each presenter will be scheduled for a total of 15 minutes (nominally a 10 minute presentation and 5 minute discussion). Please keep in mind that the time schedule is fixed so that attendees may move between sessions.
- Registration will be opened for early bird regristration before August 16, 2013 and regular registration until September 5, 2013. You can download the registration form from our website and send us by email.

We thank you for submitting this paper, for your work involved in preparing the paper and sending the final version for the publications. We look forward to your participation in ICOME 2013.

Sincerely yours,
Chairman,

Ary Bachtiar KP, PhD

Applied Mechanics and Materials

TRANS TECH PUBLICATIONS

Applied Mechanics and Materials Vol. 493

doi: https://doi.org/10.4028/www.scientific.net/AMM.493

Numerical Studies on R22 Refrigerant Compressor Using Environment Friendly Working Fluids

Authors: K.G. Sai Shreenaath, Jigar Golecha, L. Bruno Augustin, M. Suresh

Abstract: Vapour compression refrigeration is the most widely used method in domestic and commercial air conditioning and refrigeration systems. R22 (difluoromonochloromethane) is the most widely used HCFC (hydro chlorofluorocarbon) refrigerant in residential, commercial, industrial and transport cooling systems. Montreal protocol in 1987 banned the use of CFCs (chlorofluorocarbon) due to their adverse impact on the environment causing ozone depletion and global warming. HCFCs are also being phased out, though they are less destructive than CFCs. The present work explores compressor performance using alternate environment friendly working fluids so that R22 can be replaced in future. The refrigerants used for the studies are R134a (tetrafluoroethane), R290 (propane) and R600a (isobutane). Compressor performance is analysed by varying refrigerant mass flow rate, evaporator and condenser temperatures and studying their effect on compressor size, power and discharge temperature. A numerical simulation code has been developed in MATLAB using refrigerant properties taken from REFPROP.

...more

21

Case Studies Thermal Analysis of HP Condensate Stabilizer Column

Authors: Muhammad Qirom, Antonius Indarto, I. Arsa Putrawan

Abstract: The HP condensate stabilizer column is located in the condensate stabilizer unit that functions to recover light hydrocarbons from feed. The HP condensate stabilizer column is a stripping column equipped with 15 trays, condenser, reboiler and a pump-around. The main purpose of HP column is to recover propane and butane components from feed condensate by a distillation process. This process is conducted by heating the liquid in the bottom of the column using steam. The amount of heat supplied is depend on the mass and heat balance in the column based on the targeted product quality from the bottom of the column. The product quality measured is Reid Vapor Pressure (RVP) that indicate the volatility characteristics of bottom product.

...more

27

The Influence of Hydrogen Addition to Diesel Fuel Spray Combustion for Different Atomization Conditions

Authors: Nyenyep Sriwardani, Yuya Okamoto, Takehiko Seo, Masato Mikami

Abstract: The negative effects of hydrocarbon fuels are widely highlighted by increasing global warming and declining quality of human health. Therefore, it is important to reduce the level of emissions from liquid hydrocarbon combustion. Hydrogen addition to the combustion chamber is one of the proven methods to improve emssions level. In this research, an experiment was conducted on diesel fuel spray combustion with hydrogen addition. The effect of additional hydrogen was observed on CO, CO_2, NO and THC exhaust gas emissions. A small hydrogen fraction (0~3 vol %) was added to the rich premixed spray combustion. The results show that increasing the hydrogen fraction reduced the emission indexes of CO and THC, and increased the emission index of CO_2. Increasing the hydrogen fraction caused an increase in the emission

index of NO, but the actual physical amount was insignificant. Increasing the atomizing air flow rate reduced the CO and THC emission indexes, but increased the CO_2 and NO emission indexes.
...more

33

Hydrogen Production from Acetic Acid Steam Reforming over Bimetallic Ni-Co on La_2O_3 Catalyst-Effect of the Catalyst Dilution

Authors: Tuan Amran Tuan Abdullah, Walid Nabgan, Mohd Johari Kamaruddin, Ramli Mat, Anwar Johari, Arshad Ahmad

Abstract: Catalytic steam reforming of acetic acid using bimetallic catalysts of 5 wt.% nickel and 5 wt.% cobalt supported on Lanthanum (III) oxide (La_2O_3) for hydrogen production was investigated in a micro fixed bed reactor. The reactor was of quartz tube with a 10 mm inside diameter. The effect of catalyst dilution on the reaction was studied. Silicon carbide was used as the dilution material. The experiments were conducted at atmospheric pressure and temperatures ranging from 500 to 700°C. The complete conversion of acetic acid to product gases has been observed at 550°C and 700°C for diluted and non-diluted catalysts respectively. It shows that catalyst dilution had a profound effect on the conversion of acetic acid at low temperature (550°C) whilst high temperature of 700°C was required for the non-diluted catalyst. The product gas distributions are similar when using both diluted and non-diluted catalysts.
...more

39

Driving Efficiency through Hydrocarbon for Green Car Air Conditioning

Authors: Afiq Aiman Dahlan, Henry Nasution, Azhar Abdul Aziz, Zulkarnain Abdul Latiff, Mohd Rozi Mohd Perang, A.Y. Wan Mohd

Abstract: The feasibility of hydrocarbon mixtures to replace HFC-R134a in automotive air conditioning systems is investigated in this paper. The temperature distribution in car cabin and fuel consumption are evaluated at various passenger load and vehicle speeds using hydrofluorocarbons refrigerant (HFC-R134a) and hydrocarbon refrigerant as the working fluid of the compressor. The experiments are tested in an actual petrol engine vehicle on a roller dynamometer to simulate actual vehicle on level road. The experiments are conducted at the same surrounding conditions. The test has performed by varying the vehicle speed; 50, 70, 90 and 110 kph, and number of passengers; 1 and 2, at temperature set-point of 21°C. The result shows that the hydrocarbon mixtures provide excellent temperature distribution and fuel conservation effect is about 2.95% to 11.90%. In addition, the results support the possibility of using hydrocarbon mixtures as an alternative to HFC-R134a in the automotive air conditioning system, without the necessity of changing parts in the current system.
...more

45

Air to Air Ejector with Various Divergent Mixing Chambers

Authors: Václav Dvořák

Abstract: The article deals with experimental investigation of subsonic air to air ejector with various configurations of the mixing chamber and the diffuser. A constant mixing chamber, 2° and 4° divergent mixing chambers and 6° diffuser were applied to find differences in the mixing process. Characteristics of the ejector, static pressure distributions and pressure fluctuations were

measured to find how the different shape of the mixing chamber affect the efficiency of mixing processes. Pressure fluctuation increased rapidly while the ejection ratio was higher than 1.25 and the highest efficiency of the ejector was obtained when using configuration 4-4-6.
...more

50

Kamojang Geothermal Power Plant Unit-1 : 30 Years of Operation

Authors: Reza Adiprana, Danu Sito Purnomo, Iwan Setiono

Abstract: UNIT-1 KAMOJANG geothermal power plant marked the new era of renewable energy in Indonesia. With its built capacity of 30 MWe, it constantly supply electricity to Java-Bali grid for more than 30 years now.Over those period, Unit-1 has given its best performance with highest achievement on Capacity Factor (CF) and Equivalent Availability Factor (EAF).High performance geothermal power plant involves the integration not only from the point of view of power generation, but also the optimation of geothermal potention in the area. Kamojang geothermal field, which is considered as one among five steam dominated reservoir in the world produces 200 MWe of the electricity nowadays. In order to maintain this production rate, some technical consideration must be made.Towards sustainable power generation of geothermal power, some assessment has been made to turbine, generator and cooling tower to ensure its current condition. Basically what it called remaining life assessment gives a rough picture of how long the equipment will run through in its operational condition.Based on those assessment, additional 20.900 hours is given to the turbine with the existing operating conditions. On the other hand, cooling tower infrastucture test and simulation delivers operation period for another 25 years.
...more

56

Flow Visualization Pattern on Sharp Edge T-Junction through Dividing Flow Channel

Authors: Y.B. Lukiyanto, I.N.G. Wardana, Widya Wijayanti, M. Agus Choiron

Abstract: In the previous study, sharp edge T-junction had been investigated to determine head losses and flow pattern. In this study, sharp edge T-junction was used as inlet flow model scale to determine flow visualization pattern. The apparatus test provide a dividing flow channel on static conditions which is the inlet pressure larger than 1 atm. Pressure difference is measured by using a U-pipe manometer. The manometer was inserted between inlet and outlet. Flow rate is measured by collecting fluid into a measuring cup. The coefficient of losses is determined as a result for predicting the losses energy. Flow Visualization Pattern is one of solution to perform the mechanism of sharp edge T-junction as inlet flow model scale. The result shows that flow pattern from simulation has the same trend with experimental results.
...more

62

An Experimental Study on the Vertical Flow Past a Finite-Length Horizontal Cylinder at Low Reynolds Numbers

Authors: Willy Stevanus, Yi Jiun Peter Lin

Abstract: The research studies the characteristics of the vertical flow past a finite-length horizontal cylinder at low Reynolds numbers (Re_D) from 250 to 1080. The experiments were

performed in a vertical closed-loop water tunnel. Flow fields were observed by the particle tracer approach for flow visualization and measured by the Particle Image Velocimetry (P.I.V.) approach for velocity fields. The characteristics of vortex formation in the wake of the finite-length cylinder change at different regions from the tip to the base of it. Near the tip, a pair of vortices in the wake was observed and the size of the vortex increased as the observed section was away from the tip. Around a distance of 3 diameters of the cylinder from its tip, the vortex street in the wake was observed. The characteristics of vortex formation also change with increasing Reynolds numbers. At X/D = -3, a pair of vortices was observed in the wake for Re_D = 250, but as the Re_D increases the vortex street was observed at the same section. The vortex shedding frequency is analyzed by Fast Fourier Transform (FFT). Experimental results show that the downwash flow affects the vortex shedding frequency even to 5 diameters of the cylinder from its tip. The interaction between the downwash flow and the Von Kármán vortex street in the wake of the cylinder is presented in this paper.
...more

68

Effect of Air Conditioning Position on Thermal Comfort in the Floor Air Conditioning System

Authors: Y.A. Sabtalistia, S.N.N. Ekasiwi, B. Iskandriawan

Abstract: Energy consumption for air conditioning systems (air conditioning system) increased along with the increasing need for fresh air and comfortable in the room especially apartments. FAC system (Floor Air Conditioning) is growing because it is more energy efficient than CAC (Ceiling Air Conditioning) system. However, the position of the AC supply is on the lower level at the FAC system causes draft discomfort becomes greater as air supply closer to the occupants so that thermal comfort can be reduced. Heat mixture of windows, exterior walls, kitchen, and occupants in the studio apartment affect thermal comfort in the room too.This study aims to determine the position of the AC supply which has the best thermal comfort of FAC system in the studio apartment. It can be done by analyzing ADPI (Air Diffusion Performance Index), the distribution of air temperature, wind speed, RH (Relative Humidity), and DR (Draft Risk) to change the position of the AC supply supported by CFD (Computational Fluid Dynamics) simulation.This result prove that AC position 2 (on wall near the kitchen) is more comfortable than AC position 1 (on the bathroom wall) because AC position 2 away from occupied areas, thereby reducing the occurrence of draught discomfort.
...more

74

Computational Fluid Dynamic Using Parallel Loop of Multi-Cores Processor

Authors: C.L Siow, Jaswar, Efi Afrizal

Abstract: Computational Fluid Dynamics (CFD) software is often used to study fluid flow and structures motion in fluids. The CFD normally requires large size of arrays and computer memory and then caused long execution time. However, Innovation of computer hardware such as multi-cores processor provides an alternative solution to improve this programming performance. This paper discussed loop parallelize multi-cores processor for optimization of sequential looping CFD code. This loop parallelize CFD was achieved by applying multi-tasking or multi-threading code into the original CFD code which was developed by one of the authors.

The CFD code was developed based on Reynolds Average Navier-Stokes (RANS) method. The new CFD code program was developed using Microsoft Visual Basic (VB) programming language. In the early stage, the whole CFD code was constructed in a sequential flow before it is modified to parallel flow by using VBs multi-threading library. In the comparison, fluid flow around the hull of round-shaped FPSO was selected to compare the performance of both the programming codes. Besides, executed results of this self-developed code such as pressure distribution around the hull were also presented in this paper.
...more

Experimental Studies on a Solar Air Heater Having V-Corrugated Absorber Plate with Obstacles Bent Vertically

Authors: Ekadewi A. Handoyo, Djatmiko Ichsani, Prabowo, S. Sutardi

Abstract: A solar air heater (SAH) is a simple heater using solar radiation that is useful for drying or space heating. Unfortunately, heat transfer from the absorber plate to the air inside the solar air heater is low. Some researchers reported that obstacles are able to improve the heat transfer in a flat plate solar air collector and others found that a v-corrugated absorber plate gives better heat transfer than a flat plate. Yet, no work of combining these two findings is found.This paper describes the result of experimental study on a SAH with v-corrugated absorber plate and obstacles bent vertically started from 80^{o} to 0^{o} with interval 10^{o} on its bottom plate. Experiments were conducted indoor at five different Reynolds numbers (1447 Re 7237) and three different radiation intensities (430, 573, and 716 W/m^{2}).It is found that the obstacles improve SAH performance. Both the air temperature rise and efficiency increase with inserting obstacles bent at any angle vertically. Unfortunately, the air pressure drop is increasing, too. Obstacles bent vertically at smaller angle (means more straight) give higher air temperature rise and efficiency. However, the optimum angle is found 30^{o}. The air temperature rise and efficiency will be 5.3% lower when the obstacles bent 30^{o} instead of 0^{o}, but the pressure drop will be 17.2% lower.
...more

Energy Savings in Air Conditioning System Using Ejector: An Overview

Authors: Kasni Sumeru, Luga Martin, Farid Nasir Ani, Henry Nasution, Farid Nasir Ani

Abstract: There are two ejector configurations described in the present study: ejector refrigeration cycle and the ejector as an expansion device. The use of waste heat from the car engine and industry as a heat-driven energy for air conditioning system in automobile and building can save energy. Although the ejector refrigeration cycle has a low COP, the use of waste heat as a heat-driven energy incurs a lower operational cost compared with vapor compression refrigeration system. In addition, an ejector as an expansion device can be applied in the vapor compression refrigeration cycle to improve the performance system.
...more

Empirical Correlations for Sizing Adiabatic Capillary Tube Using LPG as Refrigerant in Split-Type Air-Conditioner

Authors: Shodiya Sulaimon, Azhar Abdul Aziz, Amer Nordin Darus, Henry Nasution

Abstract: This paper presents correlations for sizing adiabatic capillary tubes which serves as an expansion device in split-type air-conditioner with LPG, novel hydrocarbon (HC) mixtures of butane (HC600) and propane (HC290) as refrigerant. A homogenous two-phase flow model developed by the authors and also experimental investigation of the Liquified Petroluem Gas (LPG) refrigerant flow in adiabatic capillary tubes were used in this study. The theoretical model was used to assess various percentage compositions of these HC mixtures and validated with the experimental data. For each HC refrigerant mixture, correlations for sizing adiabatic capillary tube which contains the relevant factors, viz. capillary tube inner diameter, inlet pressure, refrigerant mass flow rate, capillary tube surface roughness and capillary tube inlet subcooling was developed. The proposed correlations were compared with the authors measured data and found to be in good agreement. Further validation was made by comparing the mass flow rates predictions of the correlations with experimental data of previous studies and found that these correlations are consistent. The correlations can be used in small vapour compression refrigeration systems working with the HC refrigerant mixtures for practical design and optimization.
...more

99

Validation of AWTSim as Aerodynamic Analysis for Design Wind Turbine Blade

Authors: I Kade Wiratama

Abstract: This paper presents the results of validation AWTSim code and this code has been used to analyze aerodynamic performance in the optimization design blade wind turbine. The validation was performed to know the accuracy of AWTSim code compared to WT_Perf by using the test wind turbine blade AWT-27. Blade AWT-27 was taken as the case for all through of this study and the design pitch angle for blade AWT-27 was 1.2° to stall (-1.2). However, in order to compare the results with available results, pitch angles 0, 1 and 2 degrees to stall were considered for simulation. The results of validation show that the predicted power curve, power coefficient and thrust by two codes are almost similar or less than 1%.
...more

105

Numerical Study on the Influence of the Corner Curvature of Circular Micropillar on Microdroplet Size via a Dewetting Process

Authors: Bambang Arip Dwiyantoro

Abstract: The influence of the corner curvature of circular micropillar on microdroplet formation by a dewetting process was numerically investigated. The diameter of the microdroplets is mainly determined by the capillary effect and viscous force contributed by the wetted surface i.e. on the top surface of micropillar magnifies, which slows down the movement of water front attached to the top surface of micropillar. The numerical simulations showed that the corner curvature of the micropillars play an important role in determining the flow pattern of the dewetting process, especially the evolution and movement of the meniscus across the micropillar before a microdroplet is formed. The water front on the top surface of micropillar with right-angle corner moves much slower than that on the micropillar with round corner. The numerical results also indicate that the curvature radius (r) on circular micropillar is one of the parameters

governing the size of the microdroplets formed on the top surface of the micropillars after the dewetting process, while the microdroplet diameter decreases with the increase of the dimensionless of curvature corner.
...more

111

Redesign ITS Central Library through Smart Building

Authors: Muhammad Junaidi, Kusriantoko Parindra, Hosta Ardhyananta, Ary Bachtiar, Anton A. Dimas

Abstract: Energy conservation is one of many technique applied to reduce the global warming effect. Sepuluh Nopember Institute of Technology (ITS) contributes to encourage energy conservation by ITS Eco Campus programs. It has so many activities, one of them is audit energy as one way to get energy efficiency in educational area. ITS central library is most accessable building both student and other academics community with total area more than 400 square matres and high occupation rate approximately 90% everyday. Energy audit techniques were carried out by an energy audit team to identify any energy conservation opportunities (ECOs). walk-through assessment and data analysis were conducted over all building zones. These levels of assessments proved that the building and its mechanical and electrical systems were improperly maintained and inefficiently operated. So that, ITS Central Library will be redesigned to be smart building by improving light intentensity level, humidity, and room temperature appropriate with ASHRAE90.1-2005. Thus exterior building like wall, glass, roof and floor will be redesigned to emphasize minimum total load. Replacement single glass to double glass reduce the load conduction and radiation through glass, approximately 2,7%.
...more

117

Optimization of Maximum Lift to Drag Ratio on Airfoil Design Based on Artificial Neural Network Utilizing Genetic Algorithm

Authors: Ismoyo Haryanto, Tony Suryo Utomo, Nazaruddin Sinaga, Citra Asti Rosalia, Aditya Pratama Putra

Abstract: . This paper deals with an alternative design method of airfoil for wind turbine blade for low wind speed based on combination of smart computing and numerical optimization. In this work, a simulation of Artificial Neural Network (ANN) for determining the relation between airfoil geometry and its aerodynamic characteristics was conducted. First, several airfoil geometries were generated through transformation of complex variables (Joukowski transformation), and then lift and drag coefficients of each airfoil were determined using CFD (Computational Fluid Dynamics). In present study, the ANN training was conducted using airfoil geometry and its aerodynamic characteristics as input and output, respectively. Therefore, lift and drag coefficients can be directly determined only by giving the airfoil geometry without having to perform wind tunnel experiment or numerical computation. Moreover, the optimization was conducted to obtain an airfoil geometry which gives maximum lift to drag ratio (C_L/C_D) for specific Reynolds number. For this purpose Genetic Algorithm (GA) was applied as optimizer. The results were validated using commercial CFD and it can be shown that the result are satisfactory with error approximately of 6%.
...more

123

Carbon Dioxide Effects on the Flammability Characteristics of Biogas

Authors: Nurkholis Hamidi

Abstract: Flammability limits and flame speed of methane-carbon dioxide-air mixtures have been studied to understand the effect of carbondioxide on the flammability characteristic of biogas. The fuel of biogas discussed in this study was made by mixing gases of methane and carbon dioxide. The carbon dioxide was varied from 0% (by volume) untill reach the flammability limit of the stoikhiometri biogas-air mixtures. The observation was done using a cubic combustion bomb with the dimension of 500 mm x 200 mm x 10 mm with the initial condition being at room temperature and atmospheric pressure. The ignitor was set at the top of combustion bomb, so the flame propagated downward. Base on the observation results, the presence of carbon dioxide in the fuel ofbiogas caused the flammability limits of biogasair mixture narrower. The biogas-air mixture was still flammable with the highest content of carbon dioxide of 62.5 %vol when the mixture was sthoichiometri. Compared to methane-air mixture, the presence of carbon dioxide in biogas caused a reduction in the flame speed. The stoichiometri mixture has the highest flame speed when the carbon dioxide was not present in the fuel. However, when the carbon dioxide was added in the fuel, the rich mixture has the highest flame speed. This is a consequence of the rich biogas-air mixture having a higher fraction of the carbon dioxide components from the fuel compared to the stoichiometri and lean biogas-air mixture. The result also indicated that at the upper limit the flame still propagated downward to closed to the endwall. However, at the lower limit (lean mixtures), the flame did not intend to propagate downward, it was just at the top and propagate sideward.

...more

129

Heat Transfer Effectiveness and Coefficient of Pressure Drop on the Shell Side of a Staggered Elliptical Tubes Bank

Authors: Utomo Kukuh W. Budi, Kamal Samsul, Suhanan, I. Made Suardjaja

Abstract: The effectiveness of heat transfer and the pressure drop coefficient of staggered elliptical tube banks are studied experimentally. The bank consists of 11 elliptical tubes of 0.75 equivalent diameter in an arrangement of 4-3-4. The major and the minor sub-axis of each tube are 24.70 mm and 12.35 mm respectively, and therefore the aspect ratio (AR) of the tube is 2.0. The geometric parameters of the bank are S_T = 24.70 mm, S_L = 37.00 mm and minimum frontal area B = 12.35 mm. Seven mid-tubes are internally heated by electrical heater of 69.6 Watt each. Experiment is conducted in a sub sonic wind tunnel and run with the wind velocities of 1 m/s 12.6 m/s which correspond with Reynolds number of = 346-6904. The results show that the effectiveness (ε) varied from 2144.44 to 15.26. It decreases exponentially at low Reynolds numbers and tended asymptotically at higher Reynolds number. The coefficient of pressure drop ($C\Delta p$) ranges from 7.21 to 4.41 decreases continuously at low Reynolds number and asymptotic at higher one.

...more

134

Experimental Study on the Effect of Reynolds Number Variation on Drag Force for Various Cut Angle on D-Type Cylinders

Authors: Astu Pudjanarsa, Ardian Ardawalika

Abstract: Experimental study on the effect of Reynolds number variation on drag force for various cut angles on D-type cylinders was performed. Five different cut angles on different cylinders were applied including: 35^o, 45^o, 53^o, 60^o, and 65^o. The free stream velocity was varied so the Reynolds number also varied.The experiment was carried out at a subsonic wind tunnel. Drag force for a cut D-type cylinder (for example 35^o) was measured using a force balance and wind speed was varied so that corresponding Reynolds number of $2.4\times10^4 \div 5.3\times10^4$ were achieved. Wind turning angle was kept at 0^o (without turning angle). This experiment repeated for other D-type cylinders.Experiment results show that, for all D-type cylinders, drag force decreased as the Reynolds number increased, then it was increased after attain minimum drag force. For all D-type cylinders and all variations of Reynolds number the drag minimum is attained at cut angle of 53^o. This value is appropriate with previous experiment results.
...more

140

Performance of Conical Diffuser on Liquid Jet Gas Ejector

Authors: Daru Sugati, Indarto, Purnomo, Sutrisno

Abstract: Liquid gas ejector uses liquid as the motive fluid and gas as the entrained fluid. The presence of gas in the liquid reduces the performance of the ejector, especially the diffuser. To observe the effect of entrained gas on the diffuser performance, a series of experiment was conducted.In this research, the motive flow rate was varied from 1.52 to 2.02 *l/s* and the entrained rate from 0.118 *l/s* to 0.944 *l/s*. Its effects on the pressure profile and pressure recovery were observed. If the entrained rate increase, the pressure of the throat upstream, as well as downstream, increase. In the diffuser, longer distance is needed for the pressure to reach its final value. Pressure recovery is mainly affected by void fraction. The higher the void fraction the lower the pressure recovery coefficient
...more

145

An Investigation into the Effect of Drag Coefficient on Overtaking of Car

Authors: S.S. Al Homoud, Dani Harmanto, Ilias Oraifige

Abstract: The purpose of this report is the effect of the drag coefficient on the car when it is travelling on the road and at different positions while overtaking. The investigation uses SolidWorks Flow simulation software to conduct CFD [. A car and truck has been designed in actual dimensions using SolidWorks. After performing the validation of the software, the simulation is performed having the car in four different positions. The results will determine the drag coefficient and how it is affected in the different positions.
...more

151

Effects of Pine Oil on Dynamics of Bubble in Froth Flotation

Authors: Warjito, Indra Pranata Al Kautsar

Abstract: Dynamics of bubble in froth flotation have been studied. The purpose of this research is to study the effects of pine oil on the dynamics of small bubble in froth flotation. Dynamics of bubble is an important parameter which determines flotation eficiency. Acrylic pipe was setup as a flotation column and equipped with image capture and lighting equipments. Later on, bubble

was generated by a nozzle. A different nozzle size and pine oil concentrations were used in this experiment. Eventually, the dynamics of the bubble were captured by camera and the images were then processed by image processing software. Therefore, bubbles size and its position can be determined. The results indicate that bubble movement can be divided into three stages: acceleration, deceleration and terminal velocity. It is also indicated that pine oil modify surface tension; hence the bubble size become smaller and its velocy decrease. Moreover, pine oil induces the bubble to reach terminal velocity faster then bubble in water wthout pine oil. Therefore, it can be concluded that pine oil affects bubble dynamics significantly.
...more

155

Study on Auto-Ignition Behavior of Lubricating Oil in a Cone Calorimeter

Authors: Muhammad Andira Mulia Siregar, Yulianto Sulistyo Nugroho

Abstract: Auto-ignition behavior of lubricating oil is studied experimentally using a cone calorimeter. Based on its Material Safety Data Sheet (MSDS), the adopted lubricating oil has a flash point temperature of 228°C, The measurement of auto-ignition behavior was carried at atmospheric pressure in range of temperature between 350°C to 550°C. In this work, the optical density of smoke resulting from the combustion process was measured at auto-ignition temperature. The result of this study shows that the auto-ignition behavior of lubricating oil is strongly depend on conditions of gas mixture, i.e. oil vapor, nitrogen, and oxygen mixtures. The lubricating oil started to ignite at irradiance temperature of cone heater at 500°C with a measured heat flux value of 16,7 kW/m^2. At lower temperatures ignition of the mixture occured by piloted igniton sources. No ignition was observed at temperature less than 350°C. At higher irradiance temperature and heat flux (550°C and 21,1 kW/m2), auto-ignition occured at shorter time to ignition and producing higher value of smokes optical density of 1 - 1.4 m^{-1}.
...more

161

Solar Driven Absorption Chiller for Medium Temperature Food Refrigeration, a Study for Application in Indonesia

Authors: I Nyoman Suamir

Abstract: Indonesia has abundant renewable energy resources. In 2005 this country, however, only consumed 0.38% renewable energy of the total energy consumption. Most of the energy sources of the country are from fossil fuels which result in high CO_2 emissions. Solar energy systems would be as an option to reduce the CO_2 emissions of this country. This paper studied the application of solar energy to provide cooling for medium temperature food refrigeration based on Indonesian weather conditions. The paper additionally analyzed the environmental impact relating to CO_2 emissions, and investigated the economical aspect. CFD-Fluent software was applied on modeling the modification of the absorption chiller generator to enable it to operate with heat from solar radiation, while F-Chart and Microsoft Excel spreadsheet were used to analyze the solar system and the economical viability of the technology. The results showed that the optimum modification of the absorption chiller was to use a jacket for heat addition. CFD modeling with Fluent using Diphyl THT as the heat transfer fluid (HTF) indicated that the system would function optimally at fluid temperature input of 180°C, whereas the optimum average temperature of the chiller generator would be 170 °C. The proposed technology was

found economically less viable for food refrigeration compared to the vapor compression cycle using R-404A but it could provide a significant impact on the environment by a reduction of 37% CO_2 emissions.
...more

167

The Effect of Water Droplet Size on the Extinguished Concentric Jet Premixed and Diffusion Flame

Authors: Mega Nur Sasongko

Abstract: The present research experimentally investigated the effect of different water droplet size on the burning behavior and extinction condition of concentric jet premixed and diffusion flame. Water droplet stream in line with flowing air from lower duct. The burning behavior of concentric jet flame was observed and the extinction of flame was gained by decreasing the flow rate of fuel until the flame exthinguised. The results showed that the burning behavior of concentric jet diffusion and premixed flame had the same tendency. Different water droplet size influenced the burning behavior of flame. Decreasing the water droplet size, luminosity of the flame became thin as well as reducing the flame height. However, the inhibition effect of water droplet was stronger for diffusion flame compared to premixed flame. For smaller water droplet size, water droplet was four times more effective for suppressing the diffusion flame than premixed flame
...more

173

Gaining the Enthalpy of Solid Yields Formation in the Process of Waste Pyrolysis

Authors: Widya Wijayanti

Abstract: An experimental study of pyrolysis method had been conducted to support the waste-to-energy program. It was very attractive method to convert the waste; cow dung and municipal solid waste in short time, only 2 hours. An appropriate pyrolyzer is required to support this process from the heat transfer mechanism and consider the chemical reaction. Therefore, the study aims to analyze the influence of different temperatures on the measured enthalpy of waste pyrolysis by means of calorimetrical measurement. The waste samples were used in experimental runs, and then the influence of temperature toward the solid yields were investigated. The enthalpy of solid yields formation would be presented by calorific/heating value of formed char/solid yields indicating an important-physical properties of fuel. The results referred that the values of solid yield enthalpy were pointed in a polynomial function indicating endothermic and exothermic reaction during pyrolysis. The different values exhibited that the solid yield enthalpy was also a temperature function, H(T). It ought to replace the H as temperature function in the heat energy balance governing equation. Consequently, the pyrolysis enthalpy could not only assume as endothermic values like in the previous investigations [6,8,1 but also establish both endothermic and exothermic values in globally pyrolysis process.
...more

179

Pipeline Leak Detection in Two Phase Flow Based on Fluctuation Pressure Difference and Artificial Neural Network (ANN)

Authors: Budi Santoso, Indarto, Deendarlianto

Abstract: Pipe network was an important part of the fluid transport infrastructure. On the other hand, the pipeline leak detection in two-phase flow using the flow and pressure parameters is very rarely studied. A system on the basis of the Artificial Neural Network (ANN) was proposed for detecting the pipeline leak for the two-phase plug flow by using the pressure difference measurement. In the present research, water-air mixture flows in pipe horizontal of 24 mm inner diameter. Artificial pipeline leak was modeled with the leak of solenoid valve on the bottom and top of pipe. Differential Pressure Transducer (DPT) was placed after the leak position and connected by the high-speed data acquisition. The fluctuations of the pressure difference signals were recorded as a time series of random data. The data of the combinations of the input flow rate, the pressure difference can be used to identify the pipeline leak in two-phase flow plug by using ANN. The results demonstrated a very good ability to the pipeline leak on two-phase flow. ...more

186

Reduction of Drag Force on a Circular Cylinder and Pressure Drop Using a Square Cylinder as Disturbance Body in a Narrow Channel

Authors: Wawan Aries Widodo, Randi Purnama Putra

Abstract: Many studies related with characteristics of fluid flow acrossing in a bluff body have been conducted. The aim of this research paper was to reduce pressure drop occuring in narrow channels, in which there was a circular cylindrical configuration with square cylinder as disturbance body. Another goal of this research was to reduce the drag force occuring in circular cylinder. Experimentally research of flow characteristics of the wind tunnel had a narrow channel a square cross-section, with implemenred of Reynolds number based on the hydraulic diameter from $5.21x10^4$ to $1.56x10^5$. Wind tunnel that was used had a 125x125mm cross-sectional area and the blockage ratio 26.4% and 36.4%. Specimen was in the form of circular cylinder and square cylinder as disturbance body. Variation of angle position was the inlet disturbance body with $\alpha = 20^0$, 30^0, 40^0, 50^0 and 60^0, respectively. The results was obtained from this study was Reynolds Number value was directly linear with pressure drop there, it was marked by increasing of Reynolds number, the value was also increasing pressure drop. Additional information was obtained by adding inlet disturbance body shaped of square cylinder on the upstream side of the circular cylinder that could reduce pressure drop in the duct and reduce drag happening on a circular cylinder. The position of the optimum angle to reduce pressure drop and drag force was found on the inlet disturbance body with angle $\alpha = 30^0$. ...more

192

Experimental Study of Drag Reduction on Circular Cylinder and Reduction of Pressure Drop in Narrow Channels by Using a Cylinder Disturbance Body

Authors: Wawan Aries Widodo, Nuzul Hidayat

Abstract: This paper present the results of drag reduction on circular cylinder and reduction of pressure drop in narrow rectangular channels by using circular disturbance body. This study focused on the phenomenon when the flow through the arrangement of the circular cylinder, separation will occur at a specific point on a circular cylinder resulting drag force. When the separation can be delayed so that the resulting drag force will be smaller. This can be done in

various ways, one of which is by using a cylinder disturbance body on the upper and lower side near the bluff body. This study will be conducted in a wind tunnel experiments which have narrow channels with a square cross-sectional area of 125 mm x 125 mm and a blockage ratio of 26.4% and 36.4%. Specimens used circular cylinder with 25 mm diameter (d/D= 0.16) and 37.5 mm (d/D= 0.107) as well as the circular disturbance body with a diameter of 4 mm. cylinder disturbance body placed on the upper and lower side with the position α=20^0 to 60^0 and spacing (δ=0.4 mm) to the main circular cylinder. Reynolds number based on the hydraulic diameter of 5.21×10^4 to 15.6×10^4. The results of this research show the effect of using circular disturbance body on circular cylinder and the characteristics of fluid flow on a narrow channel square cross section. At a certain position of the circular disturbance body provide value pressure drop reduction on narrow channels and drag reduction when compared to a single circular cylinder. From the experimental data presented in this paper it is observed that the position angle of circular disturbance body to reduce drag force on a circular cylinder and reducing the pressure drop in the channel are at angle 20^0 and 30^0 for D=25 mm, and 20^0, 30^0 and 40^0, respectively, for D= 37.5 mm then the best reduction for both cylinders are at an angle of 30^0.
...more

198

Flammability Limit and Flame Visualization of Gaseous Fuel Combustion Inside Meso-scale Combustor with Different Thermal Conductivity

Authors: Lilis Yuliati, Mega Nur Sasongko, Slamet Wahyudi

Abstract: This study experimentally investigated effect of thermal conductivity on the combustioncharacteristics of gaseous fuel inside a meso-scale combustor. Combustion characteristics that wereobserved in this research include flame visualization and flammability limit. Quartz glass, stainlesssteel and copper tubes with inner diameters of 3.5 mm were used as combustors. Stainless steel wiremesh was inserted inside meso-scale combustor as a flame holder. Liquid petroleum gas (LPG),which is common fuel use by Indonesian people, was used as a gaseous fuel. A stable blue flame wasestablished inside meso-scale combustor at the downstream of wire mesh for all combustor withdifferent thermal conductivity. Furthermore, flame color is blue for combustion of fuel lean orstoichiometric mixture, and blue-green for combustion of fuel rich mixture. Meso-scale combustorwith the highest thermal conductivity has the narrowest flame cross section area, especially at lowerreactant velocity. Vice versa, this combustor has the widest flammability limit, mainly at the higherreactant velocity.
...more

204

Energy Conversion in Compliance of Energy Self-Sufficient Village Program. Case Study: Jarak Village

Authors: Christia Meidiana, Ismu Rini Dwi Ari, Ema Pratnya Paramita

Abstract: The Energy Self-Sufficient Village (ESSV) is one of the main programs from Goverment of Indonesia (GoI) initiated in 2007 and addressed to improve the capability of rural areas to meet the local energy demand from renewable energy. The fulfillment of 60% energy demand is required in ESSV and the source of the energy must be renewable energy. Jarak Village has potentialas to be developed as an ESSV since it has 237 cattles generated manure waste can be converted into biogas. However, the actual conditions showed that the utilization of

manure waste as source of biogas is only 14% or about 124,2 kWh covering the energy demand from 40 households. The estimation of the total cattle available in the village can actually covers up to 62% energy demand. The existing numbers of cows generate 82.8 m^3 biogas equivalents to 124,2 kWh. Nevertheless, only 124,2 kWh 14% has been consumed by 40 households. It indicates that the consumption of biogas is not optimal. Therefore, the study purposes to evaluate and to estimate the capability of the village to meet the criteria of ESV. With the assumption that there is population growth 0.01%, the criteria of ESV can be fulfilled in 2014. The energy supply of ESV in 2014 is 62%. It indicates that the Jarak Village can actually meet the criteria of ESV in 2014.
...more

210

Parallel Speed-Up of Preconditioned Fractional Step Navier-Stokes Solvers

Authors: Vivien Djanali, Steven W. Armfield, Michael P. Kirkpatrick, Stuart Norris

Abstract: Parallel performance of a fractional step Navier-Stokes solver is investigated. Parallelisation is performed using Message Passing Interface, with domain partitioning. Block preconditioning is applied to the solution of the pressure Poisson equation, which is often the bottleneck in the computation of the fractional step method. Preconditioners tested are classes of incomplete matrix decompositions and sparse approximate inverses. The computational domain is decomposed into eight parts of about equal size in terms of the number of cells, and solved on eight parallel processors. Several aspects of the parallelisation, such as domain splitting directions, speed-up and scalability of the preconditioners, are discussed.
...more

215

Reactive Mixing Behavior of the Nitration of Glycerin in a Stirred Vessel at Various Perturbation

Authors: Retno Wulandari, I.N.G. Wardana, Slamet Wahyudi, Nurkholis Hamidi

Abstract: Mixing processes are best understood in turbulent flows, where, ironically they are only understood in a statistical sense. Similarly, detailed analysis of the mechanisms of the realistic mixing process in deterministic laminar flows is nearly absent from literature. This experiment was implemented to investigate the comparable performance of reactive mixing at various perturbation; including continuous, periodic and chaotic. The experiment was designed to reveal the effects of perturbations on glycerin dissolution in nitric acid in stirred vessel. The ratio of glycerin ($C_3H_5(OH)_3$) to nitric acid (HNO_3) is 1 : 3. The geometrical parameter was set to $R_1/R_2 = 37.5/7$, and an eccentricity of $\varepsilon = 18.75$ mm. The mixing time for dissolving fixed amounts of glycerin in fixed amounts of nitric acid was measured and compared to those from several different perturbations. It was found that mixing time for the exothermic reaction of glycerin nitration had been influenced by perturbations applied to fluid mixing. Comparable experiments have shown that mixing time in the glycerin-nitration reaction could be changed dramatically, along with various perturbations. This experiment results explicitly demonstrate the benefits of mixing performance from chaotic perturbations.
...more

221

Thermodynamic Analysis of Ejector as an Expansion Device on Split-Type Air Conditioner Using R410A as Working Fluid

Authors: Kasni Sumeru, Henry Nasution, Farid Nasir Ani

Abstract: Typically the split-type air conditioner uses a capillary tube as expansion device. To enhance the performance of the system, an ejector can be applied as expansion device to replace capillary tube. Based on the numerical modeling, the coefficient of performance (COP) of standard cycle using R410A as working fluid was slightly lower than that of R22. The use of an ejector as an expansion device on a split-type air conditioner using R410 increased the COP by 10.8%. Also, R410A has a lower total GWP impact compared with R22, which reduce negative impact on the environment.

...more

Experimental Investigation on the Use of Secondary Refrigerant in Freezer for Energy Savings

Authors: Aries Prih Haryono, Edi Sukamto, Sumeru, Farid Nasir Ani

Abstract: This study presents an experimental study on a freezer which has small cooling capacity. Typically a freezer uses primary refrigerant (direct cooling) to cool or freeze a product. In this study, a prototype of freezer using a compressor 250 W nominal power at 220V was designed and constructed. The freezer is operated on two conditions, that is, using primary and secondary refrigerant. R22 and R290 (propane) were used as primary refrigerant, whereas aqueous solution of propylene glycol as secondary refrigerant. Comparison of the system performance between the primary and the secondary refrigerant werepresented. Also, the experimental results showed that the use of R290 as primary refrigerant to replace R22 in the freezer could save electrical power consumption by 18.5%. Meanwhile, the use of the secondary refrigerant yielded energy savings by 33.19% compared with the primary refrigerant.

...more

Investigation of Natural Gas Composition Effects on Knock Phenomenon in SI Gas Engines Using Detailed Chemistry

Authors: Ahmad Javaheri, Vahid Esfahanian, Ali Salavati-Zadeh, Mehdi Darzi, Seyyed Mojtaba Mirsoheil

Abstract: Considering the growing role of natural gas as an alternative fuel in stationary and automobile engines and the differences in its composition, the influence of natural gas composition on knocking combustion in spark ignition gas engines is studied both experimentally and by employing detailed chemistry. A SI single cylinder gas engine with variable compression ratio has been used for experimental observations. The chemical scheme is embedded into a zero-dimensional model which employ three-zone approach. The scheme is used to simulate the post-flame heat release and pre-flame auto-ignition. The reactions in burning zone are modeled by chemical equilibrium calculations. The simulated results are in good agreement with the experimental observations.

...more

Flow Characteristics around Four Circular Cylinders in Equispaced Arrangement near a Plane Wall

Authors: A.Grummy Wailanduw, Triyogi Yuwono, Wawan Aries Widodo

Abstract: The flow characteristics around four circular cylinders in equispaced arrangement located near a plane wall were investigated experimentally. The pressure distributions on the each cylinder surface and on the plane wall were measured for a spacing ratio L/D= 1.5 (L, center to center spacing between cylinders; D, diameter) and G/D= 0.2 (G, gap spacing between cylinder surface and the plane wall) in a uniform flow at a Reynolds Number of 5.3×10^4. The 2D U-RANS numerical simulation with k-ω SST as viscous model was used to visualize the flow phenomena occured around the cylinders. The results showed that the flow tend to be biased on the upper side of cylinders configuration. It causes the stagnation at the upstream cylinders occured at lower side of cylinders and results a formation of a narrower wake behind the third cylinder and a wider wake behind the fourth cylinder.Keywords: equispaced arrangement, circular cylinders, plane wall

...more

Experimental Study on the Performance of In-Cabin Ventilation System

Authors: Abdul Latiff Zulkarnain, Cheong Weng Soon, Bambang Supriyo, Mohd Rozi Mohd Perang, Henry Nasution, Azhar Abdul Aziz

Abstract: Parking a car under the hot sun with all windows closed could increase in-cabin temperature as high as 70°C. For such situation, human occupancy will exposed to thermal shock and inconvenience when embarking the vehicle. Another concerned of this accumulated heat gain is the effect of gas emitted by the interior material which mostly is made of vinyl. These experimental studies try to look the possibilities of bringing down the temperature and hence to suit human habitation. In this study, two methods were implemented and they are by creating fresh air change and introducing evaporative cooling by generating water mist in the air flow for further enhancement of temperature drop. Fully automated control strategy was used based on in-cabin temperature activation by the assistance of electronic control unit (ECU). Observation was made and compare for original car condition and the one equipped with In-Cabin Ventilation (IVS). The result shows the car cabin temperature can reach as high as 65°C without ventilation. With fresh charged of air and evaporative cooling, temperature drops to a range of 40 to 50°C.

...more

Reduction of Energy Losses in the End Wall Junction Area through the Addition of Forward Facing Step Turbulent Generator

Authors: H. Mirmanto, Sutrisno, Herman Sasongko, D.Z. Noor

Abstract: The research is conducted in order to reduce energy losses caused by the secondary flow in the endwall junction. This phenomenon is caused by the interaction of two adjacent viscous flow (symmetric airfoil and endwall). Reduction of energy loss carried out by addition of Foward Facing Step Turbulator (FFST) in the upstream. Endwall junction area is modeled as a NACA 0015 airfoil and a flat plate. Position of FFST is at a distance L = 2/3 C upstream leading edge and a thickness d = 4% C. Free stream conditions $Re_d = 10^5$ with turbulence intensity (Tu) 5%. Research is conducted by numerical and experiment methods. Pathlines of numerical result

methods has an identic structure with "Oil Flow Visualization" of the experiment.Result of the research states that the addition of FFST can increase the turbulence intensity in the flow near the wall. So at the same angle of attact (α), the saddle point position on the leading edge has distance nearly the same but a little more towards the lower side and the separation line is wider than without FFST. Because the flow has stronger turbulence intensity, attachment line of the upper and lower sides have a better capability of following the contours of the body. So the point of separation can be delayed and blockage (energy loss) can be reduced as well. Reduction of energy loss is most effective on α=8 ° (4.16%),Keyword : Secondary flow, forward facing step, turbulent intensity.
...more

256

Biogas Potential of Co-Substrates in Balinese Biogas Plants

Authors: Daniel Nett, I. Nyoman Suprapta Winaya, I. Made Agus Putrawan, Rolf Wartmann, Werner Edelmann

Abstract: This research aims to give an overview on how to improve the biogas yeild in Balinese digester plants using various co-substrates which are available in Bali. A series testing on the digestibility of substrates were set up either in the field or in the biogas laboratory. In-field analyses like testing the CO_2-content and taking samples from digested manure were undertaken. Analyses such as dry matter (DM) and organic dry matter (oDM) determination, pH measurement and FOS/TAC were handled in the biogas laboratory. The huge number of different fruits in Bali gives a good opportunity to use their wastes like Durian hulls and Banana peelings, which can not be used anymore, as co-substrates in biogas plants. The results of these investigations allow to estimate the additional biogas yield, when adding co-substrates to a cow manure biogas plant.
...more

262

CFD Simulation of Heat Transfer in Fluidized Bed Reactor

Authors: I. Nyoman Suprapta Winaya, I. Made Agus Putrawan, I. Nyoman Gede Sujana, Made Sucipta

Abstract: This study aims to predict heat transfer from a heated bed in a gas fluidized bed using Syamlal-OBrien drag coefficient. Discrete particles model with the Navier-Stokes equation and Eulerian multiphase are used to approach heat transfer simulation. Coefficient of heat transfer which is related to Nusselt Number and volume fraction are calculated using Gunn model which was compiled from C^{++} program language. The effect of fluidization velocity variation on the heat transfer coefficient comes to the fore, indicating the heat transfer and solid volume fraction at the bed height are very dependent. Contour of solid volume fraction and temperature distribution are also presented.
...more

267

Influence of Bioethanol-Gasoline Blended Fuel on Performance and Emissions Characteristics from Port Injection Sinjai Engine 650 cc

Authors: Bambang Sudarmanta, Sudjud Darsopuspito, Djoko Sungkono

Abstract: Performance and emissions characteristics from port injection SINJAI engine 650 cc operating on bioethanol-gasoline blended fuels of 0%, 5%, 10%, 15% and 20% were investigated on water brake dynamometers with power capacity 120 hp. The properties of bioethanol were measured based on American Society for Testing Materials (ASTM) standards. Fuel consumption was measured by the time fuel consumption per 25 cc of fuel in a measuring glass whereas combustion air consumption was measured using an air flow meter. The emission parameters, exhaust gas temperature and air fuel ratio were measured using STARGAS exhaust gas analyzer. The increase of bioethanol content will increases the engine performance and reduces pollutan emission. The highest engine performance produced by E15 blended fuel with increased torsi, mean effective pressure and power output of 10,27 %, thermal efficiency 1,8% but specific fuel consumption increased approximatelly 12,42%. This condition occurs at engine speed 3000 - 3500 rpm. While the emission CO and HC emissions decreased significantly as a result of the leaning effect caused by the bioethanol addition. In this study, it was found that using bioetanol-gasoline blended fuels , the CO and HC emissions would be reduced appoximatelly by 55 and 32% Respectively.
...more

273

Improved Energy Saving for R22 Building Air Conditioning Retrofitted with Hydrocarbon Refrigerant, Study Case: Civil Engineering Department of ITS

Authors: Widyastuti, Ary Bachtiar Krishna Putra, Ridho Hantoro, Eky Novianarenti, Arrad Ghani Safitra

Abstract: Sepuluh November Institute of Technology (ITS) encourages the ECO Campus program. The program enables ITS to systematically identify, evaluate, manage and improve their environmental performance and practices. One of the program issue is energy saving in building. The energy saving effect of an air-conditioning system retrofit project is analyzed by Energy Conservation Opportunities (ECOs) Method. These ECOs are assessed in terms of their costs and benefits, and an economic comparison to rank the various refrigerants. Finally, an Action Plan is created where certain ECOs are selected for implementation. Civil Engineering Department has a responsibility to design infrastructure and green building concept planning. This department also has the largest energy consumption in this faculty comparing the other department. The energy consumption on this Department is 60829 kWh/month. The value of IKE is 13.39 per month with the largest electrical energy consumption in air-conditioning system is 57% from total consumption. The energy used of air-conditioning sytem is 523.692 kWh. The energy saving opportunities by CFC retrofitting with hydrocarbon can save its power consumption about 20%. It also saving cost and reducing the electricity bill of 1643871.838 IDR/month. The payback period of investment costs of retrofit R-22 to Hydrocarbonis about 13 month.
...more

281

The Evaluation of a Rigid Sail of Ship Using Wind Tunnel Test

Authors: Aries Sulisetyono

Abstract: This paper described the evaluation of rigid sail performances by using the wind tunnel test. The rigid sail models were developed in the three variations of shape geometry which was

having the same value of aspect ratio. The tests were performed to investigate the performances of sail models in terms of lift, drag, resultant, driving and heeling coefficient. The three sail models were tested at the variation of angle of attack such as 15^{o}, 20^{o} and 25^{o} respectively, and it was fluided by a uniform flow of air with three different speeds. The comparisons of test results were evaluated to look for which sail models had the best performance. Based on the test results, Model 2 which is a triangle shape had generated a maximal efficiency and thrust force compare to the other models.Keywords: rigid sail, wind tunnel, sailing ship, renewable energy
...more

287

High-Efficiency Shrouded Micro Wind Turbine for Urban-Built Environment

Authors: Bu Yung Kosasih, S.A. Jafari

Abstract: Shrouding (*diffuser augmented*) horizontal axis micro-wind turbine has been shown to be an effective ways to potentially increase the power output of micro wind turbine for applications in built environments. It is well understood that the degree of the performance enhancement depends on several factors including the diffuser shape and geometries, blade airfoils, and the wind condition at the turbine site. The effect of diffuser shape and geometries is reported in this paper. Computational fluid dynamic (CFD) simulations of a small wind turbine with a simple frustum diffuser shrouding have been carried out. The diffuser has been modeled with different shapes with the aim to understand the effect of length and area ratio on power augmentation phenomenon. The simulations provide some parameterized figures which present method to determine the beneficial range of frustum diffuser geometries for diffuser shrouded horizontal axis wind turbines.
...more

294

Production of Ethanol as a Renewable Energy by Extractive Fermentation

Authors: Tri Widjaja, Ali Altway, Ayu Ratna Permanasari, Setiyo Gunawan

Abstract: One issue with batch fermentation is that product inhibition causes low yields and ethanol productivity. The objective of this study was to increase the yield and ethanol productivity via continuous fermentation in a packed bed bioreactor with both an integrated extraction process and recycling of the raffinate into the fermenter. Molasses was used as the feedstock, and the immobilized cells were supported by κ-carrageenan. This process used n-amyl alcohol, 1-octanol, and 1-dodecanol as solvents. The yield and ethanol productivity increased from 8.79% to 20.03% and 34.54 g/L·h to 118.16 g/L·h for experiments using n-amyl alcohol, 9.05% to 12.67% and 35.59 g/L·h to 74.71 g/L·h, for 1-dodecanol, 8.89% to 13.45% and 34.93 g/L·h to 84.62 g/L·h, for1-octanol by increasing recycle ratio from 0 to 0.5. Based on these results, n-amyl alcohol was the best solvent for the extractive fermentation process.
...more

300

Kerosene-Water Flow Pattern in T-Junction Vertical Diameter Ratio 0.5 (Variation of Inclination Branch)

Authors: Dewi Puspitasari, Indarto, Purnomo, Khasani

Abstract: The separation is one of the important processes in exploration and production oil technology. Phase separation across T-junction with orientation vertical up branch is simplicity

method to achieve maximum efficiency, but useful information is rather limited. This paper is presented only for inlet flow pattern and T-junction flow pattern of kerosene water mixture with inlet diameter 36 mm and branch diameter 19 mm (diameter ratio 0.5) on the variation inclination branch are 30^{o}, 60^{o} and 90^{o}. Regulating flow by closing valve at downstream was done to obtain three flow resistance in the downstream. The flow pattern obtained in this study were : stratified (ST), three-layer-13 (3L-13) , three layer-2 (3L-2), and three layer-3 (3L-3). The results of the phase separation is best achieved under conditions inlet flow pattern stratified (ST) and T-junction three layer-3 (3L-3) flow pattern, angle 90 ° and downstream resistance 6471 Pa.Keywords: phase separation, T-junction, flow patterns, downstream resistance.
...more

306

Modeling and Analysis of Hybrid Shock Absorber for Military Vehicle Suspension

Authors: Harus Laksana Guntur, Wiwiek Hendrowati, Tidy Budiarto

Abstract: This paper deals with the design, modeling and analysis of a hybrid shock absorber for vehicle suspension. A specific design of frictional-electromagnetic-regenerative shock absorber is proposed. The hybrid shock absorber consists of the proposed frictional-electromagnetic-regenerative shock absorber assembled in parallel with a conventional-viscous shock absorber. The concept of hybrid shock absorber is proposed due to the following advantages: the regenerative shock absorber will recover some wasted vibration energy from the suspension into electrical energy to support the need for electrical energy of the vehicle, while the viscous shock absorber maintains the performance of suspension closed to its original suspension. The vehicle suspension system dynamic was mathematically modeled for three different types of suspension:1).Conventional suspension using viscous shock absorber; 2).Hybrid suspension using combination of 50% frictional-electromagnetic-regenerative shock absorberand50% viscous shock absorber; and 3).Full regenerative suspension using 100% frictional-electromagnetic-regenerative shock absorber. In this research, 6 wheels military vehicle (APC:Armour Personal Carrier) is chosen as the model due to the high possibility of applying regenerative suspension to the military/off road vehicle. Based on the mathematical models, performances of the vehicle suspension and the regenerated power from regenerative shock absorber (RSA) were simulated. The results were compared between the three types of suspension and discussed.
...more

315

Design Online Artificial Gain Updating Sliding Mode Algorithm: Applied to Internal Combustion Engine

Authors: Agoes Priyanto, Mohammad Javad Nekooei, Jaswar

Abstract: This paper presents an online Artificial Fuzzy sliding Gain Scheduling Sliding Mode Control (AFSGSMC) design and its application to internal combustion (IC) engine high performance nonlinear controller in the presence of uncertainties and external disturbance. The fuzzy online tune sliding function in fuzzy sliding mode controller is based on Mamdanis fuzzy inference system (FIS) and it has multi input and multi output. The input represents the function between sliding function, error and the rate of error. The output represents the dynamic estimator

to estimate the nonlinear dynamic equivalent in supervisory fuzzy sliding mode algorithm. The performance of the AFSGSMC was compared with the IC engine controller based on sliding mode control theory (SMC). Simulation results signify good performance of fuel ratio in presence of uncertainty and external disturbance
...more

321

Optimization Spring Coil Design for Orthodontic Tooth Movement

Authors: Moch. Agus Choiron, Endi Sutikno, Tri Handoko Wicaksono, Shigeyuki Haruyama

Abstract: Orthodontic tooth movement is achieved by the remodeling of alveolar bone in response to mechanical loading by using spring coil. Spring coil design was made of round stainless steel wire and usually it was custom-made design. In the previous study, the orthodontic force on 30 gram is required to move maxillary incisor during experimental tooth movement in rat. In this study, optimization new design of spring coil is developed to fulfill the requirement of orthodontic force. The design variable of new spring coil design is set on variation of angle aperture ($5^{o} \alpha 10^{o}$), hook length (10 mm *l* 20 mm) and hook diameter (0.012 inch *D* 0.014 inch). From the result, it can be produced the optimum designs which 8.9^{o} of angle aperture; 12 mm of hook length and 0.014 inch of hook diameter for fulfilling the requirement of orthodontic force on 30 gram force.
...more

327

Thermal Stress Intensity Factors of Crack in Solid Oxide Fuel Cells

Authors: Khairul Anam, Chih Kuang Lin

Abstract: Structural durability is the main focus of solid oxide fuel cells (SOFCs) development which is affected by the thermal stress caused by considerable CTE mismatch between components and thermal gradient. In this paper we investigate the thermal stress intensity factor for mode I, mode II and mode III of positive electrode-electrolyte-negative electrode (PEN) at room temperature and steady stage for an initial crack size of 10 μm. A commercial finite element analysis (FEA) was used to find the highly stressed regions in PENs and calculate the thermal stress intensity factors. The stress distributions are calculated at uniform room temperature and at steady stage with a non-uniform temperature profile. The thermal stress intensity factors are calculated for various principal directions at the location having the greatest maximum principal stress at room temperature and steady stage. The critical stress regions are identified based on the maximum principal stress at room temperature and steady stage. The maximum principal stress is of 53.45 MPa and 45.12 MPa in principal direction of-43.97° and-42.37° at room temperature and steady stage, respectively. The mixed-mode stress intensity factor including mode I, mode II, and mode III is calculated due to multi-axial thermal stresses. However, the stress intensity factor for mode I have a highest value compared to those for modes II and III. The principal direction has an effect on the thermal stress intensity factor for the critical region with the greatest maximum principal stress. All the calculated stress intensity factors in the present study are less than the corresponding fracture toughness given in the literature, ensuring the structural integrity for the given planar SOFC stack.
...more

Computer Assisted Fracture Reduction and Fixation Simulation for Pelvic Fractures

Authors: Pei Yuan Lee, Jiing Yih Lai, Chung Yi Huang, Yu Sheng Hu

Abstract: Abstract. The objective of this study is to present an integrated surgical simulation program on a personal computer for the preoperative planning of pelvic fractures. It first provides a visualization module to display 2D images and 3D model simultaneously. A semi-automatic bone segmentation module is then provided to separate the bony structures, enabling the manipulation of individual fractured bone and bone fragment. A bone reduction module is provided for the localization of the fractured bones. The simulation of plate and screw fixation is also presented, which provides useful information for determining the shape and size of the implants. Also, an example with real CT images are presented to demonstrate the feasibility of the proposed method.
...more

354

Structural Analysis of a Tracking Photovoltaic System with a Pedestal Solar Tracker

Authors: Chih Kuang Lin, Chen Yu Dai

Abstract: The structural integrity and deformation-induced misalignment of solar radiation for a tracking photovoltaic (PV) system under self-weight is investigated using a finite element analysis (FEA) approach. Gravity is applied to calculate the stress distribution and structural deformation. Misalignment of solar radiation induced by structural deformation is also calculated. Moreover, to avoid damages caused by resonance, natural frequencies of vibration for the given tracking PV system are also determined. Strain changes are measured experimentally at two selected locations in the given solar tracker during field operation for comparison with the simulation results. A reasonable agreement between the simulations and experimental measurements is found such that the constructed FEA model is validated to be effective in assessment of the structural integrity for PV systems under self-weight. No structural failure is predicted for all components in the given solar tracker under the given loading condition according to the von Mises failure criterion. An agreement in the trend of variation of misalignment and resultant displacement of PV modules is found. Considering the effect of self-weight only, the maximum misalignment of solar radiation is of 0.275^{o} at elevation angle of 45^{o} when rotating the solar tracker from 0^{o} to 75^{o}. It is expected that such a misalignment value will not cause a significant degradation of power generation for a PV system. The range of natural frequencies of the first six vibration modes for the given PV system is from 3.85 Hz to 11.4 Hz.
...more

361

New Polyhedral Elements Based on Virtual Node Method for Solid Mechanics and Heat Transfer Applications

Authors: Logah Perumal, M.I. Fadhel

Abstract: Finite element method (FEM) is a well-established method and commonly utilized to solve complex engineering problems which cannot be solved analytically. Various element types have been formulated over the years to facilitate engineering analyses using FEM. In this paper, new polyhedral elements are developed by utilizing virtual node method. This paper covers the

formulation of shape functions and integration schemes for the new polyhedral elements. These new polyhedral elements have advantages due to the nature of their shape functions which consist of monomials $u^a v^b w^c$. Integration of functions within the element can be accomplished by utilizing an exact integration technique. These polyhedral elements can be utilized to solve real 3 dimensional problems which arise in solid mechanics and heat transfer phenomena.
...more

367

Experimental Study of Vibration of Prototype Auditory Membrane

Authors: Harto Tanujaya, Satoyuki Kawano

Abstract: This experiment report the vibration of Prototype Auditory Membrane (PAM) for a novel implantable auditory membrane. PAM made of PVDF which is fabricated using MEMS technology. The vibration are measured as a response of a pulse sine wave which are applied from one of side of the membrane. The vibrations are analyzed experimentally based on the Fourier analyze theory.
...more

372

Interaction between a Crack and an Isotropic Tri-Material Media in Anti-Plane Elasticity

Authors: Alief Wikarta, Ching Kong Chao

Abstract: Solution of a crack interacting with a tri-material under a remote shear load for anti-plane elasticity problem is considered in this paper. The main purpose of this work is to study the interaction between a crack and a tri-material for anti-plane elasticity problem. This can be achieved by determination of the stress intensity factors that allow the characterization of this interaction from the point of view of linear elastic fracture mechanics. The proposed method is based on complex variable solution of a screw dislocation together with logarithmic singular integral equations. The singular integral equation is then solved numerically by modeling a crack in place of several segments. Some numerical results are performed to show the effects of material property combinations and geometric parameters on the normalized mode-III stress intensity factors. The results show that the stiffer materials may always give retardation effect on stress intensity factors when a crack approaching interfaces. On the other hand, the softer materials may always give enhancement effect on stress intensity factors.
...more

378

Split Bar Hopkinson with Springs Striker Bar Launcher

Authors: Agus Sigit Pramono, Sujarwanto, Handik Rivazani

Abstract: Research on the dynamic strength of various materials such as metallic materials, polymers, concrete has been done by many researchers. The Split Hopkinson Bar method is still used to produce a high strain rate. In this method, a striker bar is usually launched using pressurized gas. However, high security system is required to prevent leakage as the operating pressure is very high. Avoiding the use of high-pressure gas, in this study, a mechanical system of springs used to propel the Striker Bar. By varying the spring deflection of 1 cm to 8 cm, a linear Striker Bar velocity from 2.17 m/s until 19.45 m/s is obtained. Aluminum alloy Al-2024 has been tested with this tool and it is found that at the maximum Striker Bar velocity, strain rate

on the material can be reach 1132 s^{-1}, and dynamic compression yield strength increase 56% from quasi-static compression yield strength.
...more

383

Neural Network-Based Engine Propeller Matching (NN-EPM) for Trimaran Patrol Ship

Authors: Eddy S. Koenhardono, Eko Budi Djatmiko, Adi Soeprijanto, Mohammad I. Irawan

Abstract: In recent years efforts on reducing fuel consumption has become the greatest issue related to energy crisis and global warming. The reduction of fuel consumption can be obtained, if the ship propulsion could be operated in its best performance level. Generally this is done by an appropriate analysis of engine propeller matching (EPM). In this study an EPM based on neural-network method, or NN-EPM, is established to predict the best performance of main engines, leading at minimum fuel oil consumption. A trimaran patrol ship is selected as a case study. This patrol ship is equipped with two 2720 kW main engines each connected to a controllable pitch propeller (CPP) through a reduction gear. The input parameters are ship speed *V* and service margin SM, with the corresponding output parameters comprise of engine speed n_E, engine break horse power P_B, propeller pitch *P/D*, and the fuel consumption *FC*. An NN-EPM 2-20-15-4 configuration has been constructed out of 100 training data and then validated by 30 testing data. The maximum relative error between results from NN-EPM and EPM analysis is 2.1%, that is in term of the fuel consumption. For other parameters the errors are well below 1.0%. These facts indicate that the use of NN-EPM to predict the main engines's performance for trimaran patrol ship is satisfactory.
...more

388

Modeling, Prototyping and Testing of Regenerative Electromagnetic Shock Absorber

Authors: Arif Indro Sultoni, Nyoman Sutantra, Agus Sigit Pramono

Abstract: It is well fact known that automobiles are inefficient, wasting over 74% of energy stored in fuel as a heat. One important loss is the dissipation of vibration energy by shock absorbers in the vehicle suspension under the excitation of road irregularity and vehicle acceleration or deceleration. In this paper we design, characterize and test a regenerative electromagnetic shock absorber which can effectively recover the vibration from the road irregularity. Regeneration energy is main purpose of the design without omit vehicle comfort and handling. The dynamic model of the entire system of the electromagnetic shock absorber was proposed and described. The performance of the electric shock absorber obtained from simulations was compared toward the experiment results. Refers to the simulation, a quarter car will be able to harvest 45 Watt average power while passing C class roads with 50 km/h vehicle speed. A peak power of 45 Watt and average power of 11.43 Watt are attained from the prototype when oscillating speed of bench test at 0.1 m/s, the RMS value of suspension velocity when vehicle pass C class road with speed 50 km/h.
...more

395

Designing and Prototyping Surveillance Robot with Self-Protection Using Nail Gun

Authors: Novandri Sebastian, Erwin, Erny Listijorini, Dwinanto

Abstract: Designing and manufacturing / prototyping surveillance robot that has self-protection mechanism by using nail gun with VDI (Association of German Engineers) method, aims to design and create a robot that capable to conduct reconnaissance missions and protect themselves as well as immobilize the target object. The prototype robot is able to send data in the form of audio and visual through Wireless system by using Wi-Fi (Wireless Fidelity). The robot is equipped with self-protection system such as nail gun that can move in rotation and elevation, it is such an effective weapon to paralyze the targets objects if necessary. This robot is designed to maneuver on the field that has tilt angle up to 30o. Based on the test results, the robot is able to maneuver with speed 2.88 km/h on duration more than 30 minutes and be able to pass the field angle of 35o. Proximity sensors which are used as indicators of arm robots position works well on the pitch and yaw motion. Security system that is designed to shoot also works well. The most effective control radio frequency used is 2.4 GHz and the data sender system frequency is 5.8 GHz.

...more

Numerical Modelling of the Initial Stress and Upward Deflection of Glulam Beams Pre-Stresseed by Compressed Wood

Authors: Buan Anshari, Zhong Wei Guan

Abstract: A new approach to reinforce glulam timber beams has been developed by using compressed wood (CW) which is made of a lower grade wood through densification processes. In the reinforcing practice, compressed wood blocks are inserted into pre-cut holes on the top of glulam beams to produce pre-camber and to generate initial tensile and compressive stresses on the top and the bottom extreme fibre of the glulam beam. In order to optimize the size, the number and the location of CW blocks, 3-D finite element models have been developed. 3D non-linear finite element models have been developed to simulate the pre-camber of Glulam beams locally reinforced by compressed wood blocks. The models developed have also produced the initial tensile and compressive stresses at the top and bottom extreme fibres with building-up moisture-dependent swelling on the CW blocks. With the pre-camber and the initial stress state that cancel out proportions of working deflection and stresses.

...more

Modular System for Testing the Performance of Poly-Articulate Robotic Structures

Authors: Violeta Cristina Contoloru

Abstract: This paper presents a modular system for testing the performance of a poly-articulate robotic arm (snake like) with the push-pull actuation redundancy. Mechanical structure contains modules that allow testing of robots with different structures of the robotic arm (discrete hyper-redundant, continuous). Sensory system can be configured depending on the product and testing program adapting the sensors of position, velocity, time and vibrations. The monitoring system developed allows the automatic calibration of actuators and sensors, data and signal acquisition.

...more

414

Preliminary Numerical Study on Designing Navigation and Stability Control Systems for ITS AUV

Authors: Teguh Herlambang, Hendro Nurhadi, Subchan

Abstract: In this paper, the numerical study of designing on navigation and stability control system for AUV is studied. The study started by initiating hydrostatic forces, added masses, lift force, drag forces and thrust forces. Determining the hydrodynamic force which is the basic need to know the numerical case study on designing on navigation and stability control system for AUV where Autonomous Underwater vehicles (AUV). AUV is capably underwater vehicle in moving automatically without direct control by humans according to the trajectory. The result of numerical study is properly to be the reference for the next developing for AUV.

...more

420

Numerical Study of Salat Movements for Total Hip Replacement Patient

Authors: Rifky Ismail, Eko Saputra, Mohammad Tauviqirrahman, A.B. Legowo, Iwan Budiwan Anwar, J. Jamari

Abstract: Salat as a daily Muslim activitiy in praying contains several movements which are not suggested by orthopaedic doctor to be conducted by patient with total hip replacement (THR). Sujud and sitting are two movements in Salat which is recommended to be done above the chair for THR patients. There are lacks of scientific discussions about the consequences of the normal salat movement for Muslim THR patients. This paper observes the effect of these movements to the artificial hip joint in THR patient body. A three-dimensional finite element simulation is used to investigate the resisting moment, the contact pressure and the von Mises stress. An artificial hip joint model proposed by previous researcher is used in the simulations. The results show that sujud induces the impingement and plastic deformation whereas sitting is relatively safe to be conducted by THR patients. Some suggestions are also discussed with respect to the design of new artificial hip joint model which allows THR patients to conduct Salat in a normal way. The reduction of inset at the liner, the new profile at circumferential edge inner liner and the increase in the femoral head diameter can be considered as a guideline for new design of the artificial hip joint for Muslim.

...more

426

Physiological Concept: Visible Modeling for Feasible Design

Authors: Corinthias Pamatang Morgana Sianipar, Gatot Yudoko, Kiyoshi Dowaki

Abstract: Conceptual design plays an important role in design stage as an initiation to interpret an abstract idea into a design concept. However, conceptual modeling in previous engineering designs provided premature detailed modeling. Such methodologies delivered almost pure quantitative techniques to do the modeling, which have made it difficult to do agile design process for specific-purposed products. Such products require unique approach for each situation. This paper proposes physiological concept modeling to overcome such phenomenon by combining process and functional modeling with qualitative interpretation. Physiological modeling incorporates derivation to transform idea into a design concept with almost no

quantitative postulates. A case study on competition-based electric car is also provided to show an overview of application. The study concludes that there are seven steps required to do physiological modeling. The derivation can also bring flexibility for dynamic or continuous system by introducing cyclical & dynamic relationship between processes, including interventions from outside observed system and function of residue to accommodate side residues. By looking at previous techniques, this study brings a new light to produce design concept which is feasible but can be visibly modeled even by novice designers.
...more

432

Actuator Power Consumption of Active Suspension System with Override Control Strategy

Authors: Unggul Wasiwitono

Abstract: The main function of the vehicle suspension is to improve ride and handling performance. In vehicle active suspension, better ride comfort is usually required larger control input and larger suspension deflection. However, the actuator that deliver the control signal have a limitation which is commonly known as actuator saturation. There is also a structural constraint that limits the suspension deflection. In this study, an alternative approach to the vehicle active suspension system is proposed. In this approach, some separation in the controller such that one part is devoted to achieve nominal performance and the other part is devoted to constraint handling is performed. In addition, the actuator power consumption of the proposed control strategy is further investigated numerically. The simulation results show that the proposed control strategy can manage the trade-off between performance and the actuator power consumption.
...more

438

Trailing Edge Deformation Mechanism for Active Variable - Camber Wind Turbine Blade

Authors: Bu Yung Kosasih, Michael Dicker

Abstract: Blade root fatigue stress, primarily resulting from wind shear and turbulence, is a critical factor in wind turbine design. Blade mounted aerodynamic control devices have been shown to have the potential to reduce this. However, limited research exists into suitable devices, with great challenges being involved in meeting the requirements for use on large turbines. The blade designed in this work addresses this by employing a piezoceramic actuated compliant mechanism, contained within a flexible matrix composite structure. The resulting mechanism design achieves a sectional change in lift coefficient of ΔC_L +0.4 to 0.15. The performance of the blade is analysed with a quasi-steady time marching BEM model, employing optimal control. A reduction of 21.59% in the standard deviation of the flap-wise bending moment was achieved, a comparable result to previous load control investigations.
...more

444

Effect of Material and Process Parameter on Dimensions of Rolled External Threads

Authors: P.S. Chauhan, C.M. Agrawal, R.K. Dwivedi

Abstract: The work in this paper presents the effect of material and blank dimension on the dimensions ofexternal rolled threads. This paper will be helpful for the auto industry, one of the largest fastenersmarkets, that typically consumes between 2800 to 3100 fasteners in the assembly of an average familyvehicle. Externally threaded fasteners comprise the bulk of fasteners used in these applications withover 90% of being produced by thread rolling. The thread rolling process is now widelyacknowledged as the fastest and most efficient method of producing accurate external threads, withsurface finish and mechanical properties. The typical production rates are around one piece persecond. In order to ensure a perfect thread rolling process, it is important for blank of work piece to beproperly pre-machined. The size of the blank is dependent on material, surface finish, type of threadsetc. This paper describes the effect of blank material and dimensions on nominal diameter of externalrolled threads. The work has been carried out at M/s Gayatri Auto Industries on Master ReciprocatingDies Thread Rolling Machine using HSS die. Mild Steel (C 15), EN-8 (C40), and EN-47 (SpringSteel) materials have been taken as blank material for the analysis to produce M8x1.25 6g threads.The result indicates that the variation on surface roughness, carbon percentage and dimension of blankaffects significantly the nominal diameter and PCD of threads. This paper is helpful for theprofessionals to determine the accurate dimension of thread rolling blank for desired threads tominimize rejections.
...more

453

The Emergy Value Assessment of Municipal Waste Management in Yogyakarta, Indonesia

Authors: Christia Meidiana

Abstract: The emergy values of three different scenarios for the new landfill in Yogyakarta City were calculated to evaluate the sustainability and efficiency. The assessment included the environmental parameters which are Environmental Yield Ratio (EYR), Net Emergy, Environmental Loading ratio (ELR) and Emergy Sustainability Index (ESI).The calculation of emergy indices showed that treatment in landfill requires the largest emergy input for all scenarios with the percentage between 92% and 97%. Scenario 0 contains the lowest total solar emergy implying that it requires lower emergy input compared to other scenarios. Scenario 1 needs the lowest emergy investment. Meanwhile, Scenario 2 offers the highest emergy recovery contributed mainly by the output from higher scavenging rate. Scenario 2 is the best option for the municipal waste management in Yogyakarta since it meets more criteria for sustainability and efficiency.
...more

461

Evaluation of the Effect of Application of Air Jet Cooling and Cooled-Air Jet Cooling on Machining Characteristics of St 60 Steel

Authors: Rusnaldy, Norman Iskandar, Yusuf Umardani, Paryanto, Susilo Adi Widyanto

Abstract: The use of cutting fluid is to reduce the friction between tool and workpiece, reduce and dissipate generated heat. The application of cutting fluid is also to improve the surface quality of workpiece and increase the tool life. On the other side, cutting fluid contains chemical carcinogens that causes serious health risks for machine operators and have inherent waste disposal concern on the environment. Due to these problems, some alternative have been sought

to minimize or avoid the use of cutting fluid in machining processes. Air cooling techniques were proposed as alternative cooling mediums, i.e air jet cooling (AJC) and cooled-air jet cooling (CAJC), the liquid less method. In this work, air cooling techniques were investigated to be a possible solution of machining problem for cooling medium. This studi was also motivated by economics point of view that the application of AJC and CAJC would be more efficient than liquid method. The purpose of this study is to investigate the effect of AJC and CAJC on turning process of St 60 steel because it is used widely for production of components especially in small and medium enterprises in Indonesia. The tool tip temperatures, surface roughness and tool wear were measured for a range of cutting times. For a comparison purposes, experiments were also carried out with using traditional liquid coolant and without any cooling applied to the tool tip (dry cutting method). Experiments have shown that air cooling technques (AJC, and CAJC) can be used as cooling medium in machining process. Experimental results show that machining with CAJC have shorter tool life compare to machining with AJC and dry cutting, but liquid coolant in this studi is still the best cooling medium for machining of St 60 steel..
...more

Abstract: This paper presents simulation of drawing force and thickness deformation in deep drawing which employs semi-active blank holder force system, to solve the problem of cracking and wrinkling. The method of slab with feed back control failure criteria, was employed to make the modeling system and the semi-active blank holder to prevent wrinkling and cracking in forming low carbon steel sheet, without lubrication (μ=0.4). In this study, the mechanical properties of the material were chosen since that they equivalent to those of low carbon steel with its thickness of 0.2 mm, k = 572 N/mm^2, UTS = 391 N/mm^2, yield stress = 309 N/mm^2 and n = 0.2. The diameter and the depth of the cylindrical cup-shaped product were 40 mm and 10 mm, respectively. Results from simulation have shown that the semi-active blank holder system can control very responsive against changing of deformation condition. The optimum of initial blank holder force is approximately 3000 N up to 4000 N. In the early stages (initial stroke), blank holder force system could be responsive to prevent cracking, and at the end of the punch stroke, it is very effective to prevent wrinkling. Simulation of semi-active blank holder force control system is excellent in model formation to prevent cracking and wrinkling.
...more

Abstract: This research is about the system architecture for embedding of the Compact Fuzzy Logic Controller (Compact-FLC) into the FPGA with a minimal need in device resource. This exciting research is to minimize the FPGA resources needed to build Compact-FLC based on FPGA for controlling each joint of arm robots manipulator. Compact-FLC results of this research have been used in the XILINX Spartan 3 XC3S1000 FPGA.The Compact-FLC has been applied

with satisfactory results as Servo Controller for one joint of arm robot manipulator which the results showed that the controller achieved a process speed of 65,4uS, which is equivalent to a maximum sampling frequency of 15.290 KHz. Output membership function in this Compact-FLC used singleton membership function with Center Of Area algorithm. Two input membership functions, i.e E (Error) and CE (Change Error) have been used, both formed from several combination of triangular membership functions. The maximum number of fuzzysets that can be processed is sixteen. The overlapping function is not limited because there have been 256 if-then rule available as look up table in FPGA's ROM.The device utilization summary from ISE of XILINX development software gave the following data: Slice FlipFlops needed are 3869 or 25% of 15360 availability, 4 input LUT needed are 2319 or 15% of 15360 availability, Blocks of RAM needed are 4 or 16% of 24 availability, MULT18x18s needed are 2 or 8% of 24 availability, GCLKs needed are 2 or 25% of 8 availability, Bonded IOBs needed are 32 or 18% of 173 availability.
...more

480

Organizational Culture in Manufacturing Company: Study Case of Small and Medium Sized Enterprises in Central Java, Indonesia

Authors: Hanna Lestari, Rifky Ismail, Agus Mansur

Abstract: This paper discuss the organizational culture in metal manufacturing company which is classified as small and medium sized enterprises (SME) located in Central Java Province, Indonesia. This study is conducted to observe the action of the SME, especially for metal manufacturing company to face the regional free trade agreement in South-East Asia as a consequence of global market. The organizational culture is classified based on the internal factor, external factor, stability and control and flexibility and discretion. Four companies are involved in this study, where Company A, B and C are classified as small enterprises and Company D is classified as medium enterprise. The results described that the organizational culture is adhocracy for Company A, market for Company B and Company D and hierarchy for Company C. The adhocracy cultured company is predicted to be survived in ACFTA due to their innovative, customized and unique metal product and also specific customer. The medium enterprises is predicted to survive in ACFTA era due to their strong organizational structure, focused future plan, product diversification and measured product quality and standardization. The organizational culture for SMEs which is predicted to be suitable in winning ACFTA competition is adhocracy and market and supported by the product innovation, diversification and quality control. Mechanical and industrial engineers from university should takes place in assisting and supporting SMEs to win the competition in ACFTA era.
...more

486

Development Machining of Titanium Alloys: A Review

Authors: Mahros Darsin, Hari Arbiantara Basuki

Abstract: Titanium and its alloys are hard materials, wear resistant, high strength to weight ratio. Therefore this material become very promising, especially in aerospace application. However, its application restrict when face machining processes. This material is very hard which is very difficult to manufacture by machining. Its low Youngs modulus tends to springy and creates

vibration or chatter. Moreover, it has low heat dissipation rate that make the heat concentrate in the tool tip especially in the friction surface between tool and chip. Those phenomena result in very low tool life and low quality of machined surface, in term of surface roughness, surface integrity. This article describes some efforts to overcome those problems. Categorically, there are some groups of effort, i.e. varying machining parameters, modification the tool, treatment of the material, and different method of applying the coolant. It seems that using cryogenic cooling upon the tool is the most promising new technology to machine the titanium alloy.
...more

Abstract: Chatter is a self-excited vibration that occurs during machining process. It becomes a limitation to productivity and reduces the surface quality of work piece. Increasing dynamic stiffness of the work piece will improve its stability limit against chatter occurrence.Initial linear-approach simulation performing finite element modal and harmonic response analysis of the work piece filled with granular stiffener (sand and gravel) is presented. *Drucker-Prager granular frictional material model* is chosen to represent sand and gravel used as stiffener. Drucker-Prager parameters are chosen based on the experiment setting condition.Effect of an addition of the granular stiffener on the dynamic stiffness of the work piece will be evaluated. The simulation results are verified by experiment results.
...more

Abstract: The purpose of this study is illustrated the potential of applying the additive manufacturing (AM) technology with a low-cost three-dimensional (3D) printer on clinical applications of spine surgeries. First, the target vertebrae will be extracted from the computed tomography (CT) images of a patient and converted to a 3D polyhedral model. After choosing the target regions of pedicle screws in this 3D polyhedral model, the optimal screw angles and depths will be obtained without injuring the spinal cord. Then, a drill guide template of pedicle screws will be developed by using an AM software, and fabricated by a low-cost 3D printer. The doctor can utilize it to buckle the specific designed position of the vertebrae of the patient, and drill directly through the guide hole during the scoliosis surgery. These steps can reduce the surgical time substantially. Finally, several cases were executed to verify the placement accuracy of drill guide templates fabricated by the low-cost 3D printer.
...more

Abstract: 2D (two-dimensional) motion is the basic motion for computer numerical controlled (CNC) machine in all industrial applications. In this paper, it is aimed to optimize the multi-performance characteristics, namely roundness error determined by best-fit-circle (REB), actual radius (R_act) and position time (Tt) that is the time needed for making a circular motion. By applying a Taguchi Grey Proportional Integral Derivative (TGPID) control method, the performance of this 2D multi linear motion is improved. The roundness error is closed to zero as time went to infinity which means the actual radius is closed to the reference radius. The position time differences (dTt) of X and Y axis for circling is also zero. This indicated the TGPID approach is robust.
...more

Abstract: This paper proposes to understand about basic magnetic levitation model. Magnetic Levitation is repulsive or attractive force resulting gap from magnetic field. Characteristic of the magnetic levitation model is used permanent magnet and electromagnet with PID control to maintain wide gap between levitator and object levitation. Mass addition is used to analysis the model of the Maglev with PID control to maintain wide gap. Calculation result show that the maglev with PID control has sufficient levitation force in the maintain wide gap. Comparison between calculated and measured values can be done to build a another complex model magnetic levitation.
...more

Abstract: This paper propose the optimization of the wire electrical discharge machining (WEDM) process of SKD61 tool steel (AISI H13). The use of the Taguchi method combined with grey relational analysis and fuzzy logic has been applied for optimization of multiple quality characteristics. The WEDM machining parameters (arc on time, on time, open voltage, off time and servo voltage) were optimized with considerations of multiple performance characteristics, i.e., MRR, SR and kerf. Arc on time was set at two different levels while the other four were set at three different levels. Based on Taguchi method, an L_{18} mixed-orthogonal array was chosen for the experiments. Experimental results have shown that machining performance characteristics of WEDM process can be improved effectively through the combination of Taguchi method and grey-fuzzy logic.
...more

Abstract: In this study, the optimization of recast layer thickness and surface roughness (SR) simultaneously in a Wire-EDM process by using Taguchi method with fuzzy logic has been applied. The Wire-EDM process parameters (arc on time, on time, open voltage, off time and servo voltage) were optimized with considerations of multiple performance characteristics, i.e., recast layer thickness and SR. Based on the Taguchi method, an L_{18} mixed-orthogonal array table was chosen for the experiments. Fuzzy reasoning of the multiple performance characteristics has been developed based on fuzzy logic, which then converted into a fuzzy reasoning grade or FRG. As a result, the optimization of complicated multiple performance characteristics was transformed into the optimization of single response performance index. Experimental results have shown that machining performance characteristics of Wire-EDM process can be improved effectively through the combination of Taguchi method and fuzzy logic.
...more

529

Optimization of Tool Wear, Surface Roughness and Material Removal Rate in the Milling Process of Al 6061 Using Taguchi and Weighted Principal Component Analysis (WPCA)

Authors: Laily Ulfiyah, Bambang Pramujati, Bobby Oedy Pramoedyo Soepangkat

Abstract: In the metal cutting industry, end milling has an important role in cutting metal to obtain the various required shapes and size. This study takes Al 6061 as working material and investigates three performance characteristics, i.e., tool wear (VB), surface roughness (Ra) and material removal rate (MRR), with Taguchi method and WPCA for determining the optimal parameters in the end milling process. The performance characteristic of MRR is larger-the-better while VB and Ra are having smaller-the-better performance characteristic. Based on Taguchi method, an L_{18} mixed-orthogonal array was chosen for the experiments. The optimization was conducted by using weighted principal component analysis (WPCA). As a result, the optimization of complicated multiple performance characteristics was transformed into the optimization of single response performance index. The most significant machining parameters which affected the multiple performance characteristics were type of milling operation, spindle speed, feed rate and depth of cut. Experimental result have also shown that machining performance characteristics of end milling process can improved effectively through the combination of Taguchi method and WPCA.
...more

535

Design and Application of the Stretching Technology on the Welding Process of Stiffened Sheet Metal Structure

Authors: Heru Sukanto, Mesin Triyono, Nurul Muhayat

Abstract: Stiffened sheet metal structure where sheet metal is reinforced by frame has been claimed as the most effective structure because it has low volume and weight. It is generally applied to large car body structure such as bus and train body. Frame and sheet are commonly joined by welding process. Due to the local heating of welding, distortion or deformation will occur in this structure. To mitigate this distortion, new method called stretching technology was proposed in this work. In this method, sheet was stretched to certain pre-strain, kept in this condition and then welded to frame. Special equipment powered by hidroulic system was

designed to support this method. Low carbon steel SPAC specimens with dimension of 400mm, 1824mm and 3mm in width, length and thick respectively were prepared to evaluate the method. Hidroulic power was controlled to meet the sheet pre-strain variations of 0.00%, 0.05%, 0.10% and 0.15%. The distortion of the specimen was measured by dial indicator with mesh point of 50mm and shown in 2D contour chart. The study results revealed that the welding process on the sheet without pre-strain had the highest distortion of 8.34mm while that with pre-strain of 0.05% provided the lowest distortion of 3,3mm or 60% lower than without pre-strain specimen. The pre-strain of 0.10% and 0.15% produced the sheet distortion of 7.05mm and 7.9mm respectively. The excessive pre-strain was an ineffective method to mitigate the welding distortion because the reverse tension force of sheet would destroy the weld joint when the hydraulic force was released.
...more

541

Effect of High Speed Dry End Milling on Surface Roughness and Cutting Forces of Ti-6Al-4V ELI

Authors: Safian Sharif, Habib Safari, Sudin Izman, Denni Kurniawan

Abstract: The surface quality generated when high speed dry end milling (HSDEM) Ti-6Al-4V-ELI titanium alloy with coated and uncoated carbide tools were investigated. Evaluation was conducted using TiAlN+TiN coated and uncoated cemented carbide tools under different high cutting speeds and feed rates conditions. Surface roughness and cutting forces were measured when using new tools. The milled surface quality and corresponding alteration were characterized through electron microscopy. Within the investigated conditions high quality surface finish was obtained on the machined surface. Increasing cutting speed from 200 to 300 m/min during the process improved the surface finished particularly under lower feed rates. In term of generated surface quality, uncoated H25 grade carbide tools out performed coated F40M grade specifically at the higher cutting conditions. The main damages observed after HSDEM on the surface for all machining conditions contain redeposited materials, feed marks, and tool edge marks. Under both tested feed rates the resultant cutting force decreased by increasing the cutting speeds and uncoated carbide tools provide the lower cutting forces compared to coated types.
...more

546

Visible Light Maskless Photolithography for Biomachining Application

Authors: Dedi Suwandi, Yudan Whulanza, Jos Istiyanto

Abstract: Maskless photolithograpy is an alternative method of conventional UV photolithograpy for microfabrication since its advantages of time and cost saving. For this reason, a visible-light based maskless photolithograpy is proposed as a part of biomachining process. Modification of the method is done by replacing light source of UV light to visible light, utilizing commercial DLP projector and changing the material removal process that generally uses echant with biomachining process. The process was done by using the profile generated by computer then displayed through a commercial DLP projector shining speciment test. Focusing lens placed under the projector to draw the focal point and reduces the size of the profile. The best parameter was determined by setring exposure time, developing time, variation profiles, focusing, colors combination and optical aspect. Using a commercial projector maskless photolithography on a

negative resist tone successfully performed. The best characteristic was obtained by placing the focusing lens 3X magnification within 3 cm below the projector and 14 cm above speciment test, color combination of black-light blue (R = 0, G = 176, B = 240), with the timing of prebake 1 minute, exposure 7 minutes, postbake 5 minutes, developing 5 minutes produces the smallest profile 166 μm with 13,7 μm deviation. Biomachining process with bacteria Acidithiobacillus ferrooxidans NBRC 14262 on copper was also successfully performed with the smallest profile of 180 μm with 26 μm deviation.
...more

552

Improvement of Tungsten Inert Gas (TIG) Welding Penetration Using the Effect of Electromagnetic Field

Authors: Ario Sunar Baskoro, Tuparjono, Erwanto, S. Frisman, Adrian Yogi, Winarto Winarto

Abstract: Tungsten Inert Gas (TIG) welding is a process which an electric arc generated by the tungsten electrode to the workpiece and the welding area protected by a protective gas. Arc shape can be affected by electromagnetic force. In previous study, the use of some electromagnetic field around the arc has influenced the welding results. In this study, electromagnetic field generated from the solenoids was given to the welding arc. Welding process was conducted on Stainless Steel. The electromagnetic field made the arc becomes deflected. This deflection was controlled by the solenoid by activating it using a microcontroller. The results showed that the use of solenoid as a source of electromagnetic field has influenced the welding arc. Penetration produced by using a solenoid has deeper penetration than welding process without using solenoid. The increase of the welding power efficiency was 10.9% for arc current I = 80 A and 9.85% for arc current I = 90 A.
...more

558

Response of Grip Force as Effect of Electrics Power Input at Gripper Actuator of NiTi SM495 Wire

Authors: Tjuk Oerbandono, Hari Budiarto

Abstract: *Gripper is mechanism that mounted on the end of the robot arm and used to hold an object and move it to a certain position. Generally, classical gripper is equipped with the driving motor (electric, pneumatic, fluid power) to move the gripper mechanism. In this research, the function of driving motor replaced with gripper motor actuators made of Shape Memory Alloys (SMA) of Nickel Titanium (NiTi) wire type SM495. Problem studied is response of grip force of gripper to varied electrics power input that given to the actuator of gripper made of NiTi SM495 wire. This is a real experimental research using parameters electrical power input which is obtained by varying the applied electric voltage 3, 6, 9, 12 Volt and constant electric current 5 A. Linear springs with various springs constants of 0.14 N/mm; 0.49 N/mm; 0.981 N/mm; 1.308 N /mm were used for measuring grip force of gripper. The obtained data then analyzed using statistics (analysis of variance). The results showed that the electrical power which given to the NiTi based actuator significantly influenced the grip force of gripper. Keywords: actuators, electric power, grip force, gripper, Nickel Titanium, Shape Memory Alloys, SM495 wire*
...more

cutting force, feed force, surface roughness and tool flank wear. Experimental results are provided to illustrate the effectiveness of this approach.
...more

583

Numerical Simulation of Multipoint Forming with Circular Die Pins in Hexagonal Packing

Authors: Wardhani Rivai, Putu Suwarta, Budi Luwar Sanjoto, Husodo Nur, Subiyanto Hari

Abstract: Multipoint forming (MPF) in flexible forming technology. from the previous research of multipoint forming, the configuration of the upper and lower punch matrices were configured in square packing. In this paper, model of multipoint forming configuration was developed and the numerical simulation was performed to investigate the influence of the proposed pins arrangement, hexagonal packing. The packing density in hexagonal arrangement is higher than in square one. The deformation process in multipoint forming with hexagonal packing is evaluated in terms of stress and strains distribution. The results demonstrated that forming tool with hexagonal packing is more efficient than pins arranged in square packing. But dimples and wrinkles as the typical defect of multipoint forming was inevitable consequences of discontinuous contact between the punches and workpiece, appeared. The dimpling phenomenon is more present in MPF with hexagonal packing than with square packing.
...more

589

Design of Multi Gender Bicycle - As an Alternative Bike Design to Fulfill Appropriate Requirement for Urban Society in Indonesia

Authors: I. Made Londen Batan, Reinaldi Hendarto

Abstract: In the present work, a multi-gender bike, which can be used by men and women, was designed. The integrated design method is used to develop a bicycle frame. As a human transportation the frame is must be light, strong, and comfortable for rider. The frame of bicycle is built with the material of aluminum alloy T-6061 and is produced as prototype for a multi gender purpose. With 100 kg load the strength of material is calculated, and the result shows that the frame critical strength is smaller than material ultimate strength. The prototype was tested by 5 respondents who have an average weight of 68.2 kg, and height 169.4 cm. Pedal test is conducted with 5 level of speed such as 6, 8, 10, 12, and 14 mph in 6 minutes of cycling respectively. The paddle energy during cycling was determined. The results show that the paddle energy increase and follow the increasing of speed. However since 10 mph of speed the paddle energy tends to be fixed with average value of 40 kcal. Therefore the tension leg muscles before and after cycling is going together by increasing the speed. The RULA method is used for determining the ergonomic of multi-gender bicycle, and the result shows that the value of risk injury is 3, that mean the developed bike is ergonomic.
...more

594

Sol-Gel Synthesis of Zn Doped HA Powders and their Conversion to Porous Bodies

Authors: Abreeq Naqshbandi, Iis Sopyan, Gunawan, Suryanto

Abstract: The present study was aimed at fabricating porous ceramic scaffolds via polymeric sponge method for biomedical applications using as synthesized Zinc doped Hydroxyapatite (ZnHA) powders. Zn doped HA powders were prepared via sol-gel method using diammonia hydrogen phosphate [(NH4)2HPO4] and calcium nitrate tetrahydrate [Ca (NO3)2.4H2 as starting materials. The obtained powders were then used for the preparation of porous ZnHA scaffolds via polymeric sponge method. The green porous bodies so developed by impregnating cellulosic sponges with HA slurries, were subjected to sintering process at a temperature of 1300 Field-emission scanning electron microscopy (FESEM) was used to observe the surface morphology of the powder and sintered porous sample. The structure and crystallinity of (Zn)HA powder and the sintered porous samples was analyzed using X-ray diffractometer whereas Fourier transform infrared spectroscopy (FTIR) was used to determine the presence of various phases in the powder. FESEM results showed the formation of agglomerates at an increased Zn concentration. The morphology of the porous samples showed high degree of fusion and densification with an increase in Zn concentration. Preliminary mechanical testing results show that maximum compression strength of HA porous bodies was 0.12 MPa.
...more

603

Synthesis and Characterization of Zinc Oxide Nanoparticles via Self-Combustion Technique

Authors: Poppy Puspitasari, Andoko, Eddy Sutadji

Abstract: Zinc oxide (ZnO) is a unique material which has been used in many researches. However synthesizing nanosize ZnO remains a challenge. This deal with the preparation of ZnO nanoparticles was synthesized by a self-combustion technique. In the self-combustion technique, nanoparticles was obtained by heating the materials until the mixture combusts at 110°C. ZnO nanoparticles were synthesized from Zn $(NO_3)_2.6H_2O$ precursor observed in two different solvent. The first set of experiment involved dissolving Zn $(NO_3)_2.6H_2O$ in nitric acid (HNO_3) and adding ZnO, whereas for the second Ethylene Glycol ($C_2H_6O_2$) was used as the solvent. The material was stirred at 250 r.p.m continuously for 1 month and 3 days. The mixture was then heated up until it combusted at 110°C. Samples were then annealed at 400°C for 1 hour . The ZnO samples were characterized using X-Ray Diffraction (XRD), Raman Spectroscopy, and Field Emission Scanning Electron Microscope (FESEM). The XRD analysis showed major peak at 20-30 of 2 theta scale with [10, [00, and [10 plane of the wurtzite hexagonal structure for both sets of ZnO samples. Samples were observed at raman shift for 138 and 439 cm^{-1} and 141 and 443 cm^{-1} before and after annealing. Synthesized ZnO 1 resulted the morphology of single crystal nanorods with average dimensions of 18 nm wide and 154 nm long. ZnO 2 has obtained the morphology of single crystal nanosphere with average diameter of 30 nm.*Keywords:* Zinc Oxide, Ethylene Glycol, Self-Combustion Technique
...more

609

Effect of Ingredients on Flexural Strength of Friction Composite

Authors: Jamasri, Viktor Malau, Mochammad Noer Ilman, Eko Surojo

Abstract: In the present work, a friction composite material which will be used for material of train brake shoe was investigated to study the effect of ingredients on flexural strength. The

Taguchi method is used to measure relative effect of ingredients on flexural strength of composite. Taguchi L_8 orthogonal array which consists of 7 factors with 2 levels each is applied to perform experiment. Ingredients of friction composite were considered as factors or parameters and % volume for each factor was varied at 2 levels. Phenolic resin and barite ($BaSO_4$) were not included as factor. Phenolic resin was always kept constant at 30 % volume and % volume of barite ($BaSO_4$) was varied to compensate the changing of other ingredients amount. The results show that glass fiber and cast iron chip have significant effect on increasing of flexural strength of brake shoe composite. Conversely, NBR has significant effect on decreasing of flexural strength of brake shoe material. Cashew dust, Cu short wire, fly ash and graphite have insignificant effect on flexural strength. Cu short wire cant play a role as reinforcement fiber in brake shoe composite because there is weak bonding between Cu short wire and matrix.

...more

Abstract: A dielectric property study was performed across a wide range of frequencies and temperatures onring opening polymerisation of ε-caprolactone system in order to relate quantitatively their dielectric properties to microwave heating mechanisms. An analysis of the results concluded that heating mechanism of the polymerisation mixtures in a microwave field was controlled by the dielectric properties of monomer, where the monomer was the major component (>90 % volume/volume) as well as the component with highest dielectric loss and dissipation factor. The penetration depth of mixtures at 2.45 GHz was noted to increase from ~0.58 cm (at 20 C) to ~3.3 cm (at 150 °C). This small penetration depth limits the potential to achieve the successful scale up of a microwave-assisted polymerisation of ε-caprolactone in batch mode at 2.45 GHz. As a result, this will lead to inhomogeneous bulk temperature distribution within the polymerisation mixture and irreproducible chemistry. However, a fast heating rate based on a high value of dissipation factor and dielectric loss of the polymerisation mixtures shows potential to enable the reaction to be completed in a few seconds that may allow the polymerisation to be transferred to a continuous flow process. In so doing, small diameter tubular reactors can be employed hence removing this penetration depth issue. Thus, the polymerisation mixtures dielectric properties are worth to be considered to ensure the reliability and reproducibility of the microwave assisted synthesis of poly-ε-caprolactone at large scale production.

...more

Abstract: In this work, finite element (FE) model of spherical indentation has been developed and validated. The relationships between constitutive materials parameters (σ_y and n) of elastic-plastic materials, indentation P-h curves and hardness on spherical indenters has been

systematically investigated by combining representative stress analysis and FE modelling using steel as a typical model material group. Parametric FE models of spherical indentation have been developed. Two new approaches to characterise the P-h curves of spherical indentation have been developed and evaluated. Both approaches were proven to be adequate and effective in predicting indentation P-h curves. The concept and methodology developed is to be used to predict Rockwell hardness value of materials through direct analysis and validated with experimental data on selected sample of steels. The Hardness predicted are compared with the experimental data and showed a good agreement. The approaches established was successfully used to produce hardness values of a wide range of material properties, which is then used to establish the relationship between the hardness values with representative stress.
...more

628

Simple Recipe to Synthesize $BaTiO_3$-$BaFe_{12}O_{19}$ Nanocomposite Bulk System with High Magnetization

Authors: Dwita Suastiyantia, Bambang Soegijono, M. Hikam

Abstract: Barium titanate $BaTiO_3$ (BTO) - barium hexaferrite $BaFe_{12}O_{19}$ (BHF) nanocomposite could be as a raw material of multiferroic. Multiferroic is a class of materials with coupled electric, magnetic and structural order parameters that yield simultaneous effects of ferroelectric, ferromagnetism and ferroelasticity in the same material. This material has potential applications in such as spintronic devices and sensors. This work was an earlier research towards formation of multiferroic material. Knowing magnetic properties that will lead to a better understanding of magnetoelectric coupling in multiferroic material is the objective of this research.The samples were BTO and BHF prepared by sol-gel and then were mixed to synthesize composite in bulk system by a conventional techniques in various of weight fraction between BTO : BHF = 1:1 ; 1:2 and 1:3, then samples were sintered at 925°C for 5, 10 and 15 hours for each fraction respectively. Composite phase study was carried out using X-Ray Diffraction (XRD). MPS Magnet Physik EP3 Permagraph L was used to characterize magnetic properties. No residual phases were identified in the XRD analysis for all parameters. The peaks can be only indexed to $BaTiO_3$ and $BaFe_{12}O_{19}$ phases for all parameters respectively confirming the formation of a $BaTiO_3$-$BaFe_{12}O_{19}$ composite system. Barium titanate retains its tetragonal structure while barium hexaferrite exhibits hexagonal structure. For weight fraction of $BaFe_{12}O_{19}$ until 2 parts there is an increase of intrinsic coersive and saturation magnetization value. The maximum values of intrinsic coersive for samples with 5, 10 and 15 hours sintering are of 361.3 kA/m, 359.0 kA/m and 391.6 kA/m respectively and the maximum values of saturation are of 0.1515 T, 0.1516 T and 0.1414 T respectively leading to good characteristics of multiferroic materials.
...more

634

Effect of Cellulose Acetate Phthalate (CAP) on Characteristics and Morphology of Polysulfone/Cellulose Acetate Phthalate (PSf/CAP) Blend Membranes

Authors: Asmadi Ali, Rosli Mohd Yunus, Mohamad Awang, Anwar Johari, Ramli Mat

Abstract: Polysulfone (PSf) membrane is catogorized as hydrophobic membrane that easily fouled during membrane operation process. The presence of second hydrophilic polymer which added into membrane casting solutions plays a crucial role in adjusting the membrane properties.

This hydrophilic polymer was employed in hydrophobic polymer membranes in order to improve hydrophilicity and performance as well as formed antifouling ultrafiltration (UF) membranes. In this study, a hydrophilic polymer, cellulose acetate phthalate (CAP) was added into polysulfone (PSf) membrane casting solutions by blending technique to produce PSf/CAP blend membranes. Flat sheet asymmetric PSf/CAP blend membranes were prepared by wet phase inversion method. The results revealed that an increase in CAP increased the hydrophilicity properties of PSf/CAP blend membranes compared to pure PSf membrane. The significant changes in size and numbers of microvoids and macrovoids in the morphological structures of PSf/CAP blend membranes were due to CAP promote the instantaneous liquid-liquid demixing during phase inversion process.
...more

640

Analysis of Fiber Glass/Vinyl Ester Composite Subjected to Internal Pressure Loading for Compressed Natural Gas (CNG) Tube Type IV Application

Authors: Hosta Ardhyananta, Risa Nurin Baiti, Martha Adi Afrianto, Denni Kurniawan

Abstract: Natural gas in the form of compressed natural gas (CNG) has a pressure of 20 MPa. Glass fiber/vinyl ester composite has potential to be formed into a CNG tube. This study uses a numerical analysis method and tubular approching to assess composite ability to accept internal pressure loading, refered to failure criteria Tsai-Hill. The number of layers and fiber direction are chosen as independent variable. Configuration angle (+70, +25) provided a more optimal result than using a single angle. Composites are in a safe condition on 180th layer. Thus, the glass fiber composite material / vinyl ester is not recommended to apply in the CNG tube manufacture.
...more

645

Microstructure Study on Fe/Cr Based Alloys Added with Yttrium Oxide (Y_2O_3) Prepared via Ultrasonic Technique for Solid Oxide Fuel Cell (SOFC) Application

Authors: Dafit Feriyanto, Maizlinda Izwana Idris, Darwin Sebayang, Ashraf Bin Otman, Pudji Untoro

Abstract: Solid oxide fuel cells (SOFC) are the current research having several potential to obtain high efficiency, high energy–density power generation which operated at relatively higher temperature. Yttrium oxide (Y_2O_3) contributions at high temperature are accelerating to the development oxide layer of FeCr alloy. The aim of this research is to investigate the microstructure of Fe/Cr added with Y_2O_3 acting as a reactive element. The purpose is to improve macrostructure of Fe/Cr powders which can be applied at steel industry. In this study the mixing process of Fe/Cr and Y_2O_3 powder was conducted via ultrasonic treatment at a frequency of 22 kHz, and at two different holding time of 2.5 h and 3.5 h. The particle size of chromium (Cr) can be reduced by ultrasonic treatment at from 60µm to 30µm through threshing the cluster of Cr particle. It shows that the ultrasonic vibration effectively removes oxides and other contaminates on a surface coating. Therefore, homogeneity of the parent material, segregation, and uniform distribution of second phase were increased.
...more

651

Microstructure and Magnetic Properties of Barium Hexaferrite Produced by Sol Gel Auto Combustion for Radar Absorber Material (RAM) Application

Authors: Widyastuti, Endah Kharismawati, Mochamad Zainuri, Hosta Ardhyananta

Abstract: Barium hexaferrite ($BaFe_{12}O_{19}$) with hexagonal structure has been known as the high performance magnetic for Radar Absorber Material (RAM). Barium hexaferrite (BaM) was synthesized by sol gel auto combustion to get an homogeneous nanoparticle of BaM. Barium hexaferrites obtained from solution mixture between barium nitrate and ferri nitrate nonahidrat with precipitation of ion barium (Ba^{2+}) and ferri (Fe^{3+}) by solution of sodium hydroxide. Sample prepared with mol ratio of Fe / Ba 11 then added ammoniac in order that pH varies become 7,5; 9; and 11. Citric acid added in order that happen process of combustion. The stirring time was varieties by 1, 2, 3 hours. The effect of pH, stirring time, microstructure, phase,and magnetic properties were investigated using X-ray diffraction (XRD), Scanning Electron Microscope (SEM) and a vibrating sample magnetometer (VSM). The results showed that the highest coercivity was 0.6 Tesla and the smallest crystal size 414.409 nm was obtained for pH 7.5 and stirring time 2 hours. The largest magnetic saturation 55.54 emu /g was reached for pH 7.5 with stirring time 1 hour

...more

The Influence of Carboxy Methyl Cellulose (CMC) and Solution pH on Carbon Fiber Dispersion in White Cement Matrix

Authors: Ari Yustisia Akbar, Yulinda Lestari, Gilang Ramadhan, Septian Adi Candra, Eni Sugiarti

Abstract: Dispersion of carbon fiber in cement matrix is one of main challenges for fabricating carbon fiber reinforced cement based materials. In this study, the dispersion of carbon fiber was improved by pre-dispersion of carbon fiber in basic aqueous solution using different concentrations of CMC. The relationships of CMC concentration and pH solution toward carbon fiber dispersion in aqueous solution was evaluated by UVvis spectroscopy. In order to understand how carbon fiber is dispersed in cement matrix, morphology fiber carbon reinforced composite was examined. Experimental results show that aqueous solution of CMC is effective to disperse carbon fiber. In addition, dispersion of carbon fiber increases with increasing of pH of CMC solution.

...more

Effects of Heat Treatment and Titanium Nitride (TiN) Coating Deposited by Sputtering Technique PVD on Duylos 2510 Tool Steel Substrate

Authors: Viktor Malau, Subagyo Subagyo, Supriyanto

Abstract: The objective of this research is to characterize the effects of heat treatment such as quenching, tempering and TiN coating on mechanical and physical properties of duylos 2510 steel. These mechanical properties include wear rate, hardness, impact toughness, whereas physical properties are microstructures. Duylos 2510 steel is a cold work tool steel and has chemical composition (wt %) of 1C; 0,6 Cr; 0,1 V; 1 Mn; 0,25 Si and 0,6 W.Quenching process has been conducted by heating the specimens on austenite temperature of 800 °C with the soaking time of 30 minutes and then cooling these specimens in oil medium. Tempering process

was done at temperatures of 100, 200, 300, 400, 500 dan 600 °C with holding time of 2 hours.TiN coating has been deposited on substrates by sputtering technique of Physical Vapor Deposition at temperatures of 100, 150, 200 and 250 °C with sputtering time of 45 minutes. The mechanical and physical properties have been characterized by wear test, Vickers micro hardness test, Charpy impact test, and metallography test. This research was performed at room temperature and the major parameters of this research were tempering and sputtering temperatures.The results show that tempering temperature variations give significant modification of mechanical properties. In general, the Vickers micro-hardness decreases if tempering temperatures of the specimen increase. The highest Vickers micro-hardness of TiN coatings is 290 $HV_{0,01}$ for the specimen having sputtering temperature of 200 °C. Wear rate and impact energy increase if tempering temperatures increase. The results also show that the Vickers micro-hardness of coated specimens is higher than the micro Vickers hardness of non-coated specimens

...more

666

Experimental Study of Impact on Carbon-Fiber-Epoxy Composite Wing Leading Edge Structure

Authors: Nurihan Omar, Yulfian Aminanda, Jaffar S. Mohamed Ali

Abstract: This paper works on the curvature composite structure for wing leading edge application using fabric carbon/epoxy material subjected to impact loading. At first stage, rigid spherical projectile and elliptical panel with were used. The impact testing has been carried out by varying the radius of curvature, the thickness of the panel and different stacking sequence. The experimental results show the trend of specific energy absorption capability of structure in function of the radius, thickness of panel and carbon fiber directions.

...more

672

Acoustic Emission Hit Generation Behavior of Basalt Fiber High Strength Mortar under Compression

Authors: Ni Nyoman Kencanawati, Mitsuhiro Shigeishi

Abstract: Acoustic emission (AE) has been applied to study the fracture mechanics of concrete and other cementitious materials. In this paper, the AE hit generation behaviour is employed to investigate the fracture of high strength mortar containing basalt fiber under compression. A variety of amount and length of basalt fiber were used in mortar mix. Result shows that there is no significant effect observed on behavior of AE hit generation due to the differences amount and length of basalt fiber in mortar. All indicates the similar behaviour that can be described into three stages. At the second stage when maximum load starts to occur, AE hits are generated significantly indicating nucleation of many cracks. Materials failure in ductile manner since AE activities still can be recorded at long after post peak behaviour.

...more

678

Application of Myrmecodia Pendans Extract as a Green Corrosion Inhibitor for Mild Steel in 3.5% NaCl Solution

Authors: Atria Pradityana, Sulistijono, Abdullah Shahab

Abstract: The use of Myrmecodia Pendans (MP) extract as mild steel corrosion inhibitor in 3.5% NaCl media was investigated using weight loss and potentiodynamic polarization methods as well as characteristics analysis of the Fourier Transform Infra-Red (FTIR). Obtained data from weight loss and potentiodynamic polarization methods has shown the value of inhibition efficiency (% IE) is proportional toadded inhibitor concentration. Tafel constants data indicates that MP extract can act as cathodic and anodic inhibitors (type of mixed inhibitor). FTIR analysis also demonstrates the characteristics of MPextract. Occured inhibition mechanism was in the form of inhibitor adsorption process on metal surfacethat allegedly preceded by physical adsorption followed by chemical adsorption. Chemical adsorption is conceivable since metal surface scoping elevates as the increasing of inhibitor concentration.
...more

684

Al_2O_3– SiO_2 Coating by Flame Spray for Thermal Barrier Coating Application

Authors: Widyastuti, Mariani Lilis, S. Ridwan, M.A. Putrawan

Abstract: Nozzle is one crucial part of rocket. In this research, the nozzle was made by AISI 4340 coated by termal barrier coating (TBC). The TBC material is $Al_2O_3SiO_2$ composite, with different variation: Al_2O_3 20% SiO_2; 70% Al_2O_3 30% SiO_2; and 60% Al_2O_3 40% SiO_2. The aim of this research to observe the compositтion which will produce optimum adhesive strength and the most widely formed mullite phase. Mullite is an expected phase formed from composite and it has thermal resistance during 1300°C. Coating process was conducted by flame spray with variation of plies. The effect ratio, plies, microstructure, phase, and adhesive strength of TBC were investigated using Scanning Electron Microscope (SEM), X-ray diffraction (XRD),) and adhesion testing. The results showed that the highest adhesive strength was 16 MPa for 20%SiO2 with 2 plies. The highest mullite forming was TBC. After heat treatment, it was found that the mullite phases were most widely formed at a composition of TBC 30% SiO_2-70% Al_2O_3.
...more

691

Sintering of Stainless Steel Nanopowders for Micro-Component Part Applications

Authors: Sugeng Supriadi, Eung Ryul Baek

Abstract: Micro Metal Injection Molding utilizing 316 steel nanopowder with 100 nm in mean size was investigated to fabricate micro part. The nanopowder was used since its advantages to produce better surface roughness and detail structure in the micro part fabrication. During nanopowder preparation, thin oxide must be formed intentionally to avoid powder burnt before its exposed to the air during mixing with the wax binder system. Unfortunately, this oxide still exist after sintering and decrease the mechanical properties (ductility and densification) by the formation of secondary phase which detected as chrome oxide. In this paper, deep elaboration for oxide characteristics and the ways to reduce it by vary the sintering parameters and in Hydrogen atmosphere were described briefly. Here, we infer by reducing the heating rate, increasing the sintering temperature and utilizing the Hydrogen atmosphere can be effectively optimize the utilizing of nanopowder for micro part fabrication.
...more

697

Effect of Electron Beam Irradiation on Mechanical and Thermal Properties of Ethylene Vinyl Acetate/Polyamide 6/High Density Polyethylene Nanocomposite

Authors: Farizah Hamid, Suffiyana Akhbar, Ku Halim Ku Hamid, Abdul Rahman Mohd Faizal

Abstract: The effect of electron beam irradiation on mechanical properties of Ethylene vinyl acetate (EVA) with polyamide 6/high density polyethylene/HDPE-g-MAH and montmorillonite (MMT) were prepared by melt blending the characterization were investigated. The composites were characterized by Fourier Transform Infrared (FTIR) spectrophotometer and Thermogravimetric Analyzer (TGA) The samples were cross-linked by electron beam and irradiated at the dosage range of 0-200 kGy and 3.0 MeV. The mechanical properties of the samples which are tensile test and flexural test were measured by universal tensile machine whiles hardness was measured using Rockwell hardness tester. The gel content was performed to determine the formation of crosslinking and it showed improvement with increase dose up to 150 kGy. The result shows the increasing of tensile strength, tensile modulus, and hardness at the dosage 150 kGy but slightly decline at dose up to 200 kGy. Meanwhile TGA test showed that both irradiated and unirradiated samples have same trend characterization but irradiated samples are slightly more thermal stability. As a conclusion the electron beam irradiation enhance mechanical and thermal properties of ethylene vinyl acetate/polyamide 6/high density polyethylene nanocomposite.

...more

Effect of Tool Tilt Angle and Tool Plunge Depth on Mechanical Properties of Friction Stir Welded AA 5083 Joints

Authors: Nurul Muhayat, Achmad Zubaydi, Sulistijono, M. Zaed Yuliadi

Abstract: The influences of tool tilt angle and tool plunge depth on tensile properties of friction stir welded AA 5083-H116 with the thickness of 4 mm were studied. Four different values of tool tilt angle of 1□ 2°, 3°, and 4° were used to fabricate the joints. The tool plunge depths were choosen 3.85 mm, 3.90 mm and 3.95 mm. The FSW rotational speed and welding speed were 1125 rpm and 30 mm/min, respectively. The temperature, macrostructure, hardness and tensile strength of joints were compared and discussed. Results show that the increase of tool tilt angle and tool plunge depth resulted the welding temperature increase. Due to the increase of welding temperature, the hole defect become smaller. Tensile testing results indicated that the tensile strength of joints increased with increasing both the tool tilt angle and tool plunge depth.

...more

Preliminary Study of Development of HDPE/EVA/MMT/EFB Nanohybrid Biocomposite by Using Single Screw Extruder

Authors: Muhammad Syafiq Jainal, Siti Norsyarahah Che Kamarludin, Suffiyana Akhbar, Abdul Rahman Mohd Faizal

Abstract: This work study the mechanical properties (tensile, flexural and impact) of four different formulation of HDPE/EVA/MMT nanocomposite with present of 1.5 phr compatibilizer as a preliminary study before further development of HDPE/EVA/MMT/EFB nanohybrid biocomposite. The ethylene vinyl acetate (EVA) was varied from 0, 10, 20 and 30

wt%. Meanwhile the nanoclay montmorillonite (MMT) was varied from 0, 0.5, 1.0, 1.5, 2.0, 2.5 and 3.0 phr. HDPE/EVA/MMT ternary blends were prepared by melt extrusion blending technique using a single screw extruder. The result found that in absent of nanoclay MMT, the tensile and flexural properties (strength and modulus) of HDPE/EVA/1.5 phr compatibilizer were decreased as EVA amount are increased. Meanwhile in absent of EVA gave the highest tensile and flexural strength which are 38.53 MPa and 35.02 MPa respectively. However the trend is reciprocal for impact strength. The Izod impact test found that 30 wt% EVA give the highest impact strength which is 103.88 J/m , followed by 20 wt% EVA, 10wt % EVA and 0 wt% EVA which are 59.91 J/m, 38.11 J/m and 30.63 J/m respectively. This is because EVA plays a role as impact modifier. Meanwhile incorporation of nanoclay MMT improved the tensile and flexural properties but reducing the impact properties.
...more

715

Effect of Intercritical Annealing Temperature and Holding Time on Microstructure and Mechanical Properties of Dual Phase Low Carbon Steel

Authors: Alfirano, Wibawa Samdan, Hidayat Maulud

Abstract: Dual phase steels are an important advanced high strength steel, which have been widely used in the automotive industry for vehicle components requiring light weight and safety. In this study, the formation of dual phase structure with various volume fraction of martensite in a low carbon steel SS400 during intercritical annealing were investigated. It was found that intercritical annealing temperature and holding time affected the microstructure and mechanical properties of dual phase low carbon steel. The specimens were heated at intercritical annealing temperature of 750°C, 775°C, 800°C and 825°C, for holding periods of 6-18 minutes, followed by water quenching in order to get a dual phase ferrite and martensite. After quenching, it was obtained the optimal annealing conditions at 800°C with a holding periods of 10 minutes. In this condition, the tensile strength was increased up to 621 N/mm^2 or 39.24% higher than the initial condition, while the elongation decreased up to 13.8%. The hardness of specimens increased from 127.7 to 235.83 HVN or up to 84.67% higher than the initial condition. Meanwhile the volume fraction of martensite was 24.08%. The higher the temperature of the heating value of grain growth rate constant (K) increases. In addition, at the optimal poin, the value of *K* (grain growth rate constant) and *n* (Avramis exponent) were 0.263 and 0.318, respectively, with activation energy (Q) of 3.98 J/mol.
...more

721

The Influence of High Content of Silicon in Austenitic Stainless Steel to Corrosion Rate in Sulphuric Acid

Authors: Femiana Gapsari, Slamet Wahyudi, Sumawan

Abstract: This study is aimed at investigating the performance of saramet compared to other austenitic stainless steel (SS) types. Saramet is a type of austenitic SS which contains Silicon (Si) higher than others. The research treatment was divided into 2 activities which were at room temperature and high temperature. The material used were saramet, SS 304 and SS 316L. Corrosion test was conducted by using weight losing method and electrochemical. The findings

show that saramet is more resistant to corrosion compared to SS 304 and SS 316L both at high and room temperature. Saramet has better performance at high temperature.
...more

727

Optimization of Chemical Environment Condition towards Corrosion Rate of Sulfuric Acid Resistant Alloy Metal (Saramet) Using Response Surface Methodology

Authors: Slamet Wahyudi, Femiana Gapsari, Husni Awali

Abstract: This study investigates the variation of sulphuric acid concentration, temperature, and time towards the corrosion rate of saramet using response surfacemethod. Method used in this study is *true experimental research.* Sarametis material which is included into type of austenitic stainless steel which contains high amount of silicon. Starting at these past 2 years, the material has been widely used.This research used *weight loss method.* It has been found that minimum corrosion rate is achieved at concentration combination of 89.49% in 3.682 hoursandat temperature of 106,8 °C. From the variation combination, it is seen that the low concentration will decrease ion mobility corrossive ion from saramet.The long period of exposure supports the forming of passive layer which prevent the corrosive ions gets into the steel surface. As a result, corrosion rate decreases. At high temperature, steel which has high silicon content will be stable in terms of its atomic bound which therefore makes it posses high corrosion resistance.
...more

733

Effects of High Speed Tool Rotation in Micro Friction Stir Spot Welding of Aluminum A1100

Authors: Ario Sunar Baskoro, Suwarsono, Gandjar Kiswanto, Winarto Winarto

Abstract: Technology of Friction Stir Welding (FSW) is a relatively new technique for joining metal. In some cases on Aluminum joining, FSW gives better results compared with the arc welding processes, including the quality of welds and less distortion. The purpose of this study is to analyze the parameters effect of high speed tool rotation on *micro Friction Stir Spot Welding* (μFSSW) to the *shear strength* of welds. In this case, Aluminum material A1100, with thickness of 0.4 mm was used. Tool material of HSS material was shaped with micro grinding process. The spindle speed was fixed at 30000 rpm. Tool shoulder diameter was 3 mm, and a length of pin was 0.7 mm. The parameter variations used in this study were the variable of pin diameter (1.5 mm, 2.0 mm, and 2.5 mm), a variable of *plunge speed* (2 mm/min, 4 mm/min, 6 mm/min), and the variable of *dwell time* (2 seconds, 4 seconds, 6 seconds). Where the variation of these parameters will affect to the mechanical properties of welds (as response) was the *shear strength*. *Response Surface Methods* (RSM) was used to analyze μFSSW parameters with the *shear strength* of welds. From the result of experiment and analysis, it is shown that the important welding parameters in high speed μFSSW process are pin diameter and plunge speed.
...more

739

Slump Flow Modeling of Self-Compacting Concrete Using Smooth Support Vector Regression (SSVR)

Authors: Yoyok Setyo Hadiwidodo, Santi Wulan Purnami

Abstract: A new method of prediction based on smooth support vector regression (SSVR) is introduced to resolve the slump flow modelling of self-compacting concrete (SCC). The slump flow is a function of the content of all concrete ingredients, including cement, silica fume, water, superplasticizer, coarse and fine aggregate. In this paper, the basic ideas underlying SSVR are reviewed, and the potential of the SSVR for multiple regression (modelling) problems is demonstrated by applying the method to model of slump flow from experimental data. The results of experimentation indicate that SSVR has excellent performance on slump flow prediction. Compared with traditional prediction method such as second order regression, SSVR has much more accurate and effective to prediction of slump flow and it is very promising result.
...more

743

Hydrophobic Silica Coating Based on Waterglass on Copper by Electrophoretic Deposition

Authors: Eka Setyowatia, S.F. Amalia, Nazriati, Samsudin Affandi, Minta Yuwanae, Heru Setyawan

Abstract: Hydrophobic silica coating on copper (Cu) has been successfully prepared byelectrophoretic deposition (EPD) of silica sol prepared from waterglass. trimethyl chlorosilane (TMCS) was used as the modifying agent to produce hydrophobic coating by replacing the silanol groups on the silica surface with alkyl groups. The hydrophobicity was indicated by the contact angle of water droplet on the coating surface. It has been shown that TMCS concentration plays an important role in the preparation of hydrophobic coating. However, higher concentration of TMCS made the copper corroded before coated with silica due to the production of Cl-ions when TMCS reacted with water and silanol groups during electrophoretic deposition. In addition, the electricfield intensity, silica concentration and deposition time also influence the hydrophobicity of the coating. Increasing the three parameters produces silica coating with higher hydrophobicity. Thecontact angle of the silica coating can reach 130°. EIS analysis showed that the silica coating is very porous.
...more

749

Comparison of AISI 316L Plasma Nitriding Behavior in Low and Medium Temperature

Authors: Istiroyah, I.N.G. Wardana, D.J. Santjojo

Abstract: Plasma nitriding is a widely used technique to improve the mechanical properties and tribological properties of AISI 316L steel because it has many advantages over other surface treatment techniques. One of this advantage is plasma nitriding allows nitrogen introduce to steel at low temperature (below 500°C).In this study, nitriding of an AISI 316L was performed in high density plasma nitriding system using 70%N_2:30%H_2 gas mixture at 400°C and 480°C for 2, 4, and 8 hours. Optical Emission Spectroscopy (OES) with optical probe was used for plasma diagnosis. The properties of nitrided sample were investigated through microhardness measurement. The results show that N_2 ions and radicals are species predominantly formed in plasma.
...more

755

Na_2SO_4 Induced Hot Corrosion of Aluminized Low Carbon Steel at 700 °C

Authors: Mohammad Badaruddin

Abstract: The oxidation kinetics of hot-dip aluminized AISI 1020 steel with Na_2SO_4 deposit was investigated at 700 °C for 49 h in static air. The scale morphologies were observed by means of metallograpy, scanning electron miscroscopy (SEM), electron dispersive spectroscopy (EDS) and X-ray analyses. The accelerated oxidation of aluminized steel was attributed to the formation of aluminum-sulphides which allowed the rapid diffusion of Fe ions in the aluminide layer to the formation of iron oxide. In addition, the Al-sulphides precipitations in the alumina scale causes the Al-depletion such that Al_2O_3 layer fails to form a protective layer. Consequently, the kinetics rate of aluminized was increased.

...more

Development and Evaluation of Nano Electret Filters for Household Water Treatment

Authors: Young Chull Ahn, Jae Ik Cho, Si Eun Kim, Ah Hee Jeong, Gil Tae Kim

Abstract: Korea is expected to one of countries with water shortages, and thus must secure high-quality water resources and strictly maintain them. However, water is frequently polluted and there is still a lack of water treatment technologies and facilities to provide safe water. To remove pollutants, membrane-based methods are being widely used for water treatment. It needs high pressure and energy to capture the pollutants by pore size. In this study, electrostatic force is used to increase the efficiency of filtration and decrease pressure loss. By electro spinning, nanoelectret filter is made with 100 nm in diameter and positive charge potential. Surface potential is measured by electrostatic voltmeter system with nanoelectret filter by three conditions of applied voltage. For the filtration performance, filtration efficiency is measured by filter test system with 0.5 and 1.0 PSL. Also pressure loss of nanoelectret filter is measured by comparing PC membrane.

...more

Effect of Starter Defect to G_{IIC} of Unidirectional CFRP Composite

Authors: Fethma M. Nor, H.Y. Lee, J.Y. Lim, M.N. Tamin, Denni Kurniawan

Abstract: Critical strain energy release rate in CFRP composites characterizes the delamination resistance. More study is still needed to measure the critical strain energy release rate in sliding shear mode (G_{IIC}) considering various factors that influence its measurement. This study evaluates one of the influencing factors, the starter defect. Two types of on thin, unidirectional CFRP composites with one having thin film insert as starter defect and another one with pre-crack under Mode II loading were prepared and tested in three point bending end notch flexure (3ENF) test. It was found that the (G_{IIC}) of the former was more than twice higher than that of the latter, supposedly due to the presence of resin rich region in the former.

...more

Effect of Heat Treatment on Microstructure Homogeneity of Zn-3Mg Alloy

Authors: M.S. Dambatta, Sudin Izman, Hendra Hermawan, Denni Kurniawan

Abstract: The Zn based alloy has a high potential to be the next generation of biodegradable implant material. Development of this biomaterial involves casting process which often associated with various defects. In this study, Zn-3Mg alloy was prepared using conventional casting method and followed by homogenization treatment (370°C for 10hr) with the aim to improve the microstructure uniformity. Microscopic images show that as-cast Zn-3Mg alloy consists of segregated Zn-rich structure of star-like dendritic shape and eutectic mixture of Mg_2Zn_{11} phase. It is observed that after the heat treatment process thissegregation has been dispersed well and results in a more uniform microstructure of Zn-3Mg alloy with low fraction of casting defects.
...more

Applied Mechanics and Materials Vol. 493 (2014) pp 86-92
Online available since 2014/Jan/08 at www.scientific.net

doi:10.4028/www.scientific.net/AMM.493.86

Experimental Studies on a Solar Air Heater Having V-Corrugated Absorber Plate with Obstacles Bent Vertically

Ekadewi A. Handoyo[1,2,a], Djatmiko Ichsani[1,b], Prabowo[1,c], Sutardi[1,d]

[1]Mechanical Engineering Dept, Institut Teknologi Sepuluh Nopember, Surabaya – Indonesia
[2]Mechanical Engineering Dept, Petra Christian University, Surabaya – Indonesia
[a]ekadewi@peter.petra.ac.id, [b]djatmiko@me.its.ac.id, [c]prabowo@me.its.ac.id, [d]sutardi@me.its.ac.id

Keywords: solar air heater, obstacle, solar collector, v-corrugated absorber plate.

Abstract.

A solar air heater (SAH) is a simple heater using solar radiation that is useful for drying or space heating. Unfortunately, heat transfer from the absorber plate to the air inside the solar air heater is low. Some researchers reported that obstacles are able to improve the heat transfer in a flat plate solar air collector and others found that a v-corrugated absorber plate gives better heat transfer than a flat plate. Yet, no work of combining these two findings is found.

This paper describes the result of experimental study on a SAH with v-corrugated absorber plate and obstacles bent vertically started from 80^o to 0^o with interval 10^o on its bottom plate. Experiments were conducted indoor at five different Reynolds numbers ($1447 \leq Re \leq 7237$) and three different radiation intensities (430, 573, and 716 W/m^2).

It is found that the obstacles improve SAH performance. Both the air temperature rise and efficiency increase with inserting obstacles bent at any angle vertically. Unfortunately, the air pressure drop is increasing, too. Obstacles bent vertically at smaller angle (means more straight) give higher air temperature rise and efficiency. However, the optimum angle is found 30^o. The air temperature rise and efficiency will be 5.3% lower when the obstacles bent 30^o instead of 0^o, but the pressure drop will be 17.2% lower.

Introduction

As a country located in Equator, there is a lot of sunshine on surfaces in Indonesia. The sun's radiation energy can be converted into thermal energy by means of a solar collector. The sunlight transmitted by cover glass falls onto a plate which absorbs the heat. This absorber plate transfers the heat to the working fluid which is either water or air. Water has better thermal storage and higher convective heat transfer coefficient than air. Yet, air is much lighter and less corrosive than water. Furthermore, the heated air can directly be used for drying some farming product such as grain. Generally, the solar air heater is less efficient than the solar water heater, because air has less thermal capacity and less convection heat transfer coefficient. These encourage some research in solar air heater (SAH).

Most of SAH being investigated is flat plate type. It has a cover glass on the top, insulation on the sides and bottom to prevent heat transferred to the surrounding, a duct for the air flowing and an absorber flat plate. The air can flow over and/or under the absorber plate. To increase the convection heat transfer from the absorber plate to the air, a v-corrugated plate is used instead of a flat plate. SAH with a v-corrugated absorber plate can reach efficiency 18% higher than the flat plate under the same operation and condition [1]. A solar collector with a v-corrugated absorber is 10–15% and 5–11% more efficient in single pass and double pass modes, respectively, compared to the flat plate collectors [2]. For the same length of collector, mass flow rate, and air speed, it was found out that the corrugated and double cover glass collector gave the highest efficiency [3]. The results of mathematical simulation and experiment show that v-corrugated absorber was found to be more efficient than flat plate collector [4]. The corrugated surfaces give a significant effect on the enhancement of heat transfer and pressure drop. The Nusselt number of flow in a v-corrugated channel can increase to 3.2 – 5.0 times higher than in a plane surfaces while the pressure drop 1.96 times higher than on the corresonding plane surface [5]. The corrugated channel gave higher Nusselt

number than the straight channel and a higher channel height gave higher Nusselt number for the flow with the same Reynolds number [6].

Besides increasing the heat transfer surface area, some also give effort to increase turbulence inside the channel with fins or obstacles. The result of experimental study done in turbulent flow regime (Reynolds number of 5000 to 25,000) showed that multiple 60° V-baffle turbulator fitted on a channel provides the drastic increase in Nusselt number, friction factor, and the thermal enhancement factor values over the smooth wall channel [7]. From the research of two kinds of rectangular fins which dimension are different but total area are the same, it was found that collector with fins type II, both free and fixed, was more effective than type I and flat-plate collector. The fixed fin collector was more effective than free fin collector [8]. The efficiency of collector and the air temperature was found increasing with the use of baffles. Baffles should be used to guide the flow toward the absorber plate [9]. The experiment and theoretical investigations gave result that heat transfer was improved by employing baffled double-pass with external recycling and fins attached over and under absorber plate [10]. The obstacles on the flat plate reduced the grape drying time, because they ensure a good air flow over the absorber plate, create the turbulence and reduce the dead zones in the collector [11]. From research on three-passages SAH with three different type obstacles placed on absorber plates, it was found that type III obstacles with flow in middle passage gave the highest efficiency and all collectors with obstacles gave higher efficiency than the flat plate [12]. The optimal value of efficiency was obtained for SAH with Type II obstacles on absorber plate in flow channel for all operating conditions and the collector with obstacles appears significantly better than that without obstacles [13]. The delta-shape obstacle mounted on the absorber surface enhances the heat transfer to the air and the heat transfer was higher if the obstacle was taller and its longitudinal pitch was smaller [14].

There are two findings that are important. First, the obstacles are able to enhance heat transfer in a flat plate collector and second, a v-corrugated plate gives better heat transfer than a plane duct. It is necessary to study the combination of these two findings. Since pressure drop is an important parameter in SAH, it is interesting to study the effect of bending the obstacles vertically, too. This paper describes the result of experimental study on a SAH with v-corrugated absorber plate and obstacles bent vertically on its bottom plate.

Experimental set-up

A small scale model of a SAH having v-corrugated absorber plate has been set up indoor. Its schematic view and photograph are shown in Fig. 1. The experiments were conducted in a laboratory of Mechanical Engineering Dept of Petra Christian University, Surabaya, Indonesia.

The solar collector's model was constructed with its bottom plate can be replaced with other plate having obstacles on it. The dimension of the model was 900 mm x 90 mm x 125 mm. The cover of the collector was made of a single 3-mm transparent-tempered glass. Black painted aluminum was used as the v-corrugated absorber plate. The apex angle of the v-corrugated plate was 20^o. The dimension of the absorber plate was 900 mm long, 87 mm hypotenuse, and 0.8 mm thick. The v-corrugated duct's cross section dimension was 30 mm width and 85 mm height. To prevent heat loss, the left and right walls of collector are insulated with a 25-mm Styrofoam each and a 35-mm Styrofoam for the bottom. The obstacles used were isosceles triangular plate with dimension are 18 mm wide and 51 mm height. The ratio of spacing to height of obstacles in sequence, S/H, equal to 1 or the percentage of air flow blockage in the channel was 36% when the obstacles are straight. Thus, there are 17 obstacles. In the experiment, the obstacles were bent vertically with angle started from 80^o to 0^o with interval 10^o. Obstacles with angle 0^o mean they are straight, not bent. Thus, there are nine set of obstacles inserted on the bottom plate as shown in Fig. 1 (d).

The experiments were set up indoor to ensure the same radiation intensity, wind's speed and ambient temperature. So, a bias result that effected by different outdoor condition can be avoided. The artificial sunlight was modeled by four 500-Watt halogen lamps. A pyranometer (Kipp & Zonen, type SP Lite2) placed on top of the cover glass was used to measure the radiation intensity received on the collector. To ensure the homogenous intensity and to generate some different intensity received

on the collector, these lamps were equipped with adjustable turner individually. The experiments were conducted on three different radiation intensities, i.e. 430, 573, and 716 W/m^2.

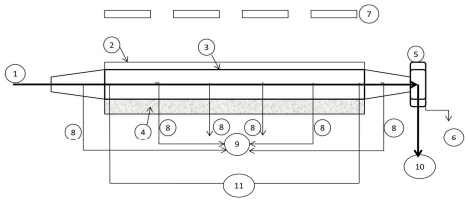

(a) Schematic of experimental set-up.

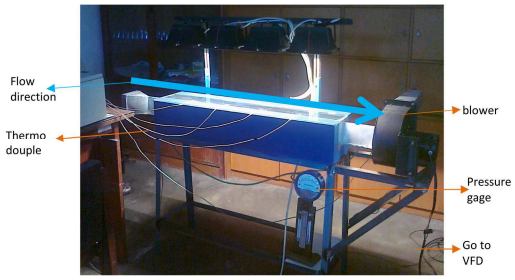

(b) Photograph of the experimental set-up

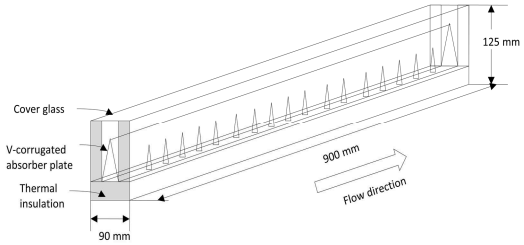

(c) Isometric view of duct

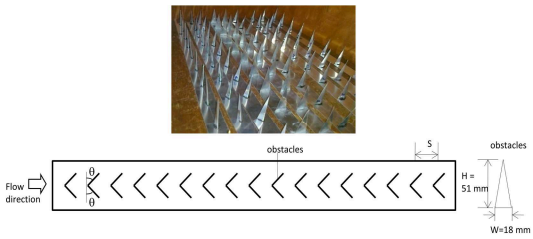

(d) top view of duct and obstacles and photograph of obstacles

Fig. 1. Experimental set-up.

The temperature, humidity, and wind speed of air surrounding were well controlled. Some T–type thermocouple which accuracy are 0.1^{o}C are used to measure temperature of flowing air at inlet and outlet of the collector, temperature of the absorber plate (at four different locations). Each thermocouple has its own display. The pressure drop between inlet and outlet of the flowing air across the collector was also measured with a Magnehelic differential pressure gage which accuracy is 2 Pa and manometer using oil which accuracy is 1 mm. A centrifugal blower was used to induce the air flowing in the channel (1000 m^3/h, 580 Pa, 0.2 kW, 380 Volt input). The air flow speed was controlled by adjusting the motor's frequency using a variable-frequency drive (VFD). The experiments were performed at five different air inlet velocities, i.e. 1.0 m/s, 2.0 m/s, 3.0 m/s, 4.0 m/s, and 5.0 m/s or at Reynolds number of 1447, 2895, 4342, 5790, and 7237, respectively. The air speed was measured using digital anemometer which accuracy is 0.1 m/s.

The experiment was conducted on model without any obstacle and consecutively with obstacles bent with some angles. Thus, there are ten set experiments conducted for each air flow speed and radiation intensity. A VFD was used to adjust the frequency of the blower's motor to ensure a constant air flow speed during the experiment.

When the inlet and outlet temperature (T_i, T_o, respectively) and the mass flow rate of air ($\dot{m}_f$) are known from experiments and the value of air specific heat (c_p) is known, then the useful energy rate ($\dot{Q}_u$) can be calculated using Eq. (1).

$$\dot{Q}_u = \dot{m}_f c_p (T_o - T_i). \quad (1)$$

According to [15], this useful energy can be expressed in terms of energy absorbed by the plate from radiation received (I) and energy lost from the absorber, as given by Eq. (2).

$$\dot{Q}_u = F_R \tau\alpha A_C I - F_R U_L A_C (T_i - T_a). \quad (2)$$

The instantaneous efficiency of a collector relates the useful energy to the total radiation received on the collector surface as shown in Eqs. (3) and (4) [15].

$$\eta = \frac{\dot{Q}_u}{I\, A_c} = \frac{\dot{m}_f c_p (T_o - T_i)}{I\, A_c} \quad (3)$$

$$\eta = \frac{\dot{Q}_u}{I\, A_c} = F_R(\tau\alpha) - F_R U_L \frac{(T_i - T_a)}{I}. \quad (4)$$

In Eq. (4), the useful energy depends on parameters of construction material of the SAH and flow conditions, i.e. F_R, the collector heat removal factor, U_L, total heat loss coefficient, A_C, collector area, and ($\tau\alpha$), transmitivity of the glass cover times absorptivity of the absorber plate.

The inlet air temperature, T_i, usually equals to the ambient temperature, T_a, during experiments. Thus, Eq. (4) is modified to be Eq. (5) [15].

$$\eta = \frac{\dot{Q}_u}{I\,A_c} = F_o\tau\alpha - F_o U_L \frac{(T_o - T_a)}{I}. \quad (5)$$

Eq. (5) specifies that a plot of instantaneous efficiency as a function of $\frac{(T_o - T_a)}{I}$ will result a straight line which slope and intercept are $F_o U_L$, and $F_o \tau\alpha$. F_o is the collector heat gain factor. If the optical properties of the SAH, ($\tau\alpha$), are known, then F_o and U_L can be determined.

Results and discussion

The experiments were conducted on three different radiation intensities and five different air flow speed. The performance of SAH includes the air temperature rise, instantaneous efficiency, and air pressure drop. The air temperature rise is determined from ($T_o - T_i$) and the instantaneous efficiency is calculated using Eq. (5). The pressure drop is measured directly during experiments.

The radiation received on the absorber plate and the air flow rate crossing the SAH affect the rise of air temperature as shown in Fig. 2. It is higher when the air flow is lower at any radiation intensity and when the radiation intensity is larger at any air flow speed. Without any obstacle, SAH gave the lowest air temperature rise of 12.7°C and the highest of 25.2°C. The lowest air temperature rise is obtained at the lowest radiation intensity (430 W/m^2) and the largest air flow speed (5.0 m/s). The highest rise is acquired at the largest radiation intensity (716 W/m^2) and the smallest air flow speed (1.0 m/s). Obstacles increase the air temperature rise whether they are bent or straight. The straight (0° obstacles) increase the lowest air rise from 12.7°C to 16.2°C and the highest air rise from 25.2°C to 34.9°C.

The air temperature rise in Fig. 2 and SAH's instantaneous efficiency in Fig. 3 decrease as the obstacles bent at larger angle. Fig. 2 show that the air temperature rise is almost the same when the obstacles bent at 30°, 20°, 10°, or 0° (straight) but the pressure drop is quite different as shown in Fig. 4. The air temperature rise and efficiency will be 5.3% lower when the obstacles bent 30° instead of 0°, but the pressure drop will be 17.2% lower.

Obstacles inserted in the flow generate turbulence and focus the air flow toward the absorber plate. When the obstacles slightly bent vertically, the air flow becomes obstructed. Some of the air will flow back causing the flow to recirculate and will reattach downstream before the next obstacles. This creates vortex near the obstacles and increase the turbulence in the air flow. Some of the air will flow in the small gap between the obstacles and absorber plate. This small gap forces the air to stay in contact with the absorber plate and to increase its velocity and turbulence. These make the heat transfer to the air flow and air pressure drop through collector increase when there are obstacles slightly bent vertically. There is something unpredictable happened, i.e. when the air flow is small (1.0 and 2.0 m/s), the temperature rise is very low as the obstacles bent at angle 10° at any radiation intensity. This phenomenon needs further research and numerical study or visualization to learn the flow around the 10° obstacles.

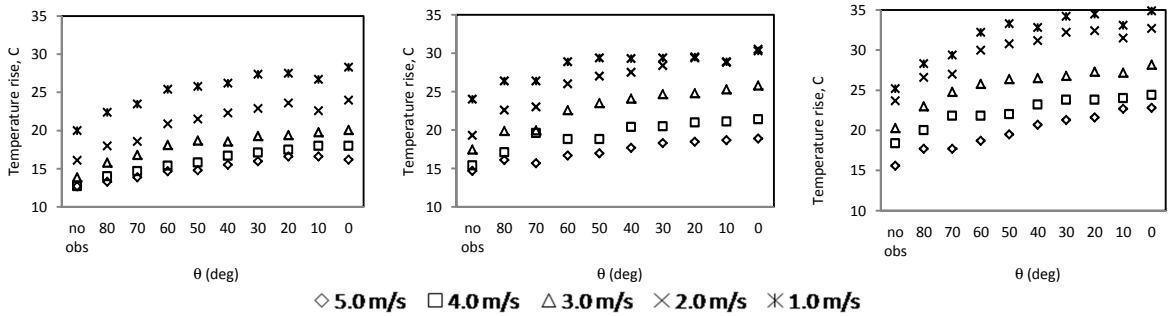

(a) 430 W/m^2 (b) 573 W/m^2 (c) 716 W/m^2

Fig. 2. The rise of air temperature at some air flow and radiation intensity for many configurations.

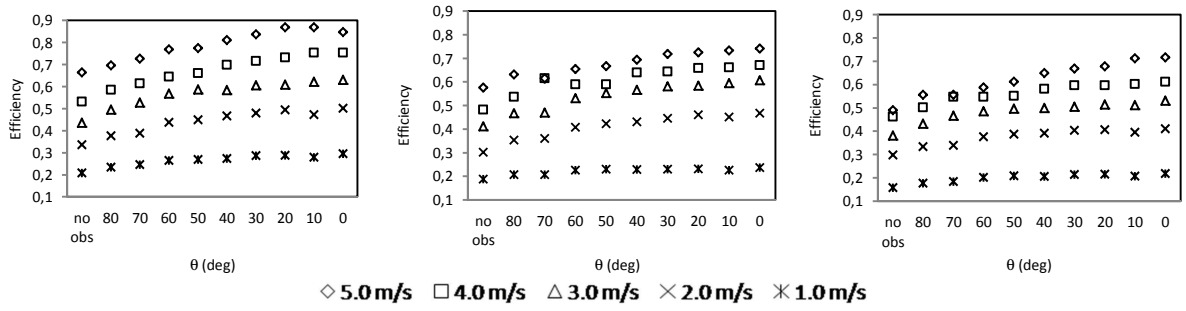

(a) 430 W/m^2 (b) 573 W/m^2 (c) 716 W/m^2

Fig. 3. Efficiency of SAH at some air flow and radiation intensity for many configurations.

The efficiency of the collector calculated using Eq. (3) shown in Fig. 3 give the consistent result with Fig. 2. As air temperature rise increased, the efficiency of the collector having obstacles also improved. For example, when inlet air speed is 5.0 m/s and radiation is 573 W/m^2, the efficiency of solar air heater with straight obstacles can reach 0.742 (74.2%) while it was only 00.577 (57.7%) when no obstacle used. The efficiency has the same trend with temperature rise, i.e. it is almost the same when the obstacles bent at 30^o, 20^o, 10^o, or 0^o (straight).

The static pressure of the air drops as it flows through the channel made by the v-corrugated absorber plate and the bottom plate. Fig. 4 shows the pressure drop for the ten SAH. To see the pressure drop more clearly, the graphs are separated, one for air flow speed of 1.0 and 2.0 m/s as in Fig. 4 (a), and one for air flow speed of 3.0 m/s, 4.0 m/s, and 5.0 m/s as in Fig. 4 (b). The pressure drop can decrease 17.2% when the obstacles bent at 30 degree instead of 0 degree when the air flow speed 5.0 m/s.

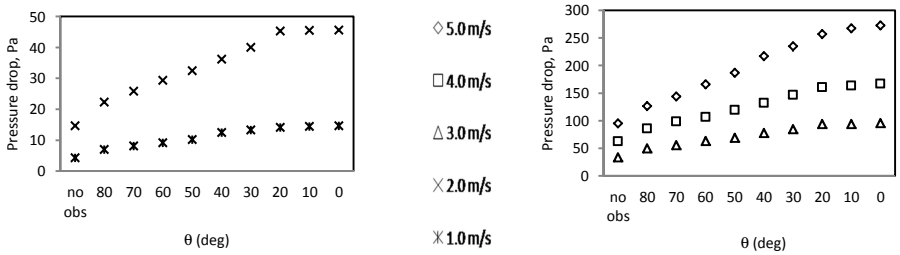

(a) Air flow speed of 1.0 and 2.0 m/s (b) Air flow speed of 3.0, 4.0, and 5.0 m/s

Fig. 4. Average pressure drop of air at different air flow speed and configuration.

The efficiency of SAH can be calculated using Eq. (5) as shown if Fig. 5. Due to space limitation, only two configurations of ten (no obstacle and 0^o obstacles) are shown. When some 0^o obstacles are inserted on the bottom plate, the efficiency is much higher than without obstacles. The slope of the linear regression is F_oU_L, and the intercept with vertical axis is $F_o\tau\alpha$.

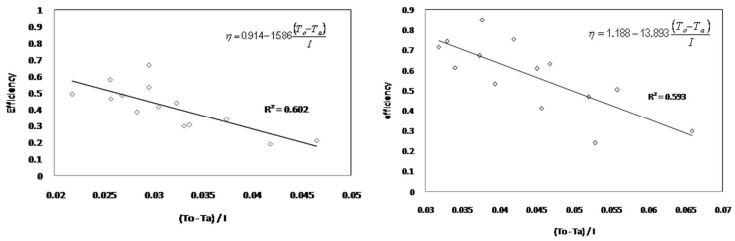

(a) No obstacle (b) 0^o obstacles

Fig. 5. Efficiency of SAH with the temperature parameter $(T_o - T_a)/I$ at two configurations.

Using data that transmissivity (τ) of tempered glass is 0.87 and absorptivity (α) of aluminum plate is 0.92, then the collector heat gain factor (F_o) and the total heat loss coefficient (U_L) can be calculated as shown in Fig. 6. SAH without obstacle has the lowest F_o and the maximum U_L. The heat gain factor (F_o) increases and total heat loss coefficient (U_L) decreases as the obstacles bent at smaller angle. Yet, the value is not quite different when the angle is 30^o, 20^o, 10^o or 0^o. The F_o decreases as much as 4% and the U_L increases as much 3.5% when the obstacles bent at 30 degree instead of 0 degree.

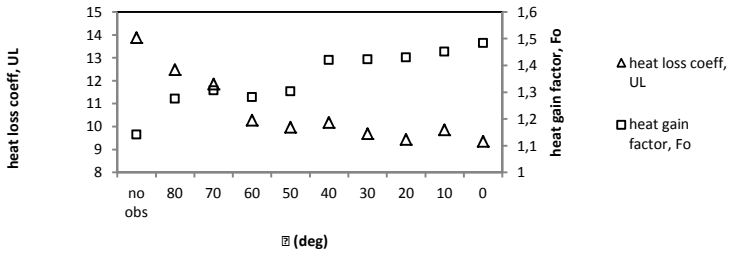

Fig. 6. The heat loss coefficient and heat gain factor of SAH with many configurations.

Conclusion

In the experimental study conducted, ten configuration of SAH were observed and compared. Following conclusions can be drawn:

- Obstacles placed on the bottom plate in a SAH with v-corrugated absorber plate improve the SAH performance. Both the air temperature rise and efficiency increase with inserting obstacles bent at any angle vertically. Unfortunately, the pressure drop is increasing, too.
- Obstacles bent vertically at smaller angles (means more straight) give higher air temperature rise and efficiency. However, the optimum angle is found 30^o. The air temperature rise and efficiency will be 5.3% lower when the obstacles bent 30^o instead of 0^o, but the pressure drop will be 17.2% lower.

Acknowledgement
Here, I am very grateful for the support from Kopertis Wilayah VII Jawa Timur, Kementerian Pendidikan dan Kebudayaan by providing Research Grant under contract no: 0004/SP2H/PP/K7/KL/II/2012.

References

[1] L. Tao, X. L. Wen, F. G. Wen and X. L. Chan, "A Parametric study on the termal performance of a solar air collector with a V-groove absorber," *Int. J. of Green Energy, 4,* p. 601–622, 2007.

[2] M. A. Karim and M. N. A. Hawlader, "Performance Investigation of Flat Plate, V-Corrugated and Finned Air Collector," *Energy 31,* pp. 452-470, 2006.

[3] C. Choudhury and H. P. Garg, "Design Analiysis of Corrugated and Flat Plate Solar Air Heaters.," *Renewable Energy Vol I, No. 5/6,* p. p. 595 – 607, 1991.

[4] A. A. Bashria, N. M. Adam, S. M. Sapuan and M. Daud, "Prediction Of The Thermal Performance Of Solar Air Heaters By Internet-Based Mathematical Simulation," *Proc. of the Institution of Mechanical Engineers,* p. 579 – 587, 2004.

[5] P. Naphon, "Heat transfer characteristics and pressure drop in channel with V corrugated upper and lower plates," *Energy conversion and management 48,* p. 1516 – 1524, 2007.

[6] Y. Islamoglu and C. Parmaksizoglu, "The effect of channel height on the enhanced heat transfer characteristics in a corrugated heat exchanger channel," *Applied Thermal Engineering 23,* p. 979–987, 2003.

[7] P. Promvonge, "Heat transfer and pressure drop in a channel with multiple 60° V-baffles," *Int. Com. in Heat and Mass Transfer,* vol. 37, p. 835–840, 2010.

[8] I. Kurtbas and E. Turgut, "Experimental Investigation of Solar Air Heater with Free and Fixed Fins: Efficiency and Exergy Loss," *Int. J. of Science & Technology,* vol. Volume 1, no. No 1, pp. 75-82., 2006.

[9] B. S. Romdhane, "The air solar collectors: Comparative study, introduction of baffles to favor the heat transfer," *Solar Energy,* vol. 81, p. 139 – 149, 2007.

[10] C.-D. Ho, H.-M. Yeh and T.-C. Chen, "Collector efficiency of upward-type double-pass solar air heaters with fins attached," *Int. Com. in Heat and Mass Transfer,* vol. 38, p. 49–56, 2011.

[11] A. Abene, V. Dubois, M. Le Ray and A. Oagued, "Study of a solar air flat plate collector: use of obstacle and application for the drying of grape," *J. of Food Engineering,* vol. 65, p. 15 – 22, 2004.

[12] H. Esen, "Experimental energy and exergy analysis of a double-flow solar air heater having different obstacles on absorber plates," *Building and Environment,* vol. 43, p. 1046–1054, 2008.

[13] E. K. Akpinar and F. Koçyiğit, "Experimental investigation of thermal performance of solar air heater having different obstacles on absorber plates," *Int. Com. in Heat and Mass Transfer,* vol. 37, p. 416–421, 2010.

[14] A. Bekele, M. Mishra and S. Dutta, "Effects of Delta-Shaped Obstacles on the Thermal Performance of Solar Air Heater," *Hindawi Publishing Corporation: Advances in Mechanical Engineering,* vol. 2011, p. 10 pages, 2011.

[15] J. A. Duffie and W. A. Beckman, Solar Engineering Of Thermal Processes, 2nd ed., John Wiley & Sons, Inc., 1991.

Advances in Applied Mechanics and Materials
10.4028/www.scientific.net/AMM.493

Experimental Studies on a Solar Air Heater Having V-Corrugated Absorber Plate with Obstacles Bent Vertically

10.4028/www.scientific.net/AMM.493.86

UNIVERSITAS KRISTEN PETRA

Ekadewi Handoyo <ekadewi@petra.ac.id>

ICOME2013 notification for paper 69

1 message

ICOME2013 <icome2013@easychair.org> Tue, Jul 9, 2013 at 12:13 AM
To: Ekadewi Handoyo <ekadewi@peter.petra.ac.id>

Dear author(s) of paper ID #69, Ekadewi Handoyo,

Based on the results of your paper's review, we would like to send the notification of acceptance of your manuscript entitled Experimental Studies on a Solar Air Heater Having V-Corrugated Absorber Plate with Obstacles Bent Vertically .

Your submission is ACCEPTED for oral presentation at the conference and publication with following revisions (if any).

Revision shall be performed according to the given comments, in order to be published in the conference proceeding and journal article. Revised paper must be submitted no later than July 31, 2013 in MS Word file.

For overseas participants, please do not hesitate to contact us should you require supporting letter for visa application.

Sincerely yours,
ICOME 2013

---------- REVIEW 1 ----------
PAPER: 69
TITLE: Experimental Studies on a Solar Air Heater Having V-Corrugated Absorber Plate with Obstacles Bent Vertically
AUTHORS: Ekadewi Handoyo, Djatmiko Ichsani, Prabowo and Sutardi

---------- REVIEW ----------
-The paper is recommended to be accepted for oral presentation. Minor correction can be made by the editor, however.
- All Figs are too small & unclear, please redraw the figures, but still concern about the max page number is 6

---------- REVIEW 2 ----------
PAPER: 69
TITLE: Experimental Studies on a Solar Air Heater Having V-Corrugated Absorber Plate with Obstacles Bent Vertically
AUTHORS: Ekadewi Handoyo, Djatmiko Ichsani, Prabowo and Sutardi

---------- REVIEW ----------
1. Fig. 1(c) is so unclear, please re-draw it for clarity.
2. Page 5, typo: only 00.557(57%) should be corrected to 0.557(57%)
3. Considering the whole paper, the manuscript was discussed physically and justified very well.
The end.

---------- REVIEW 3 ----------
PAPER: 69
TITLE: Experimental Studies on a Solar Air Heater Having V-Corrugated Absorber Plate with Obstacles Bent Vertically
AUTHORS: Ekadewi Handoyo, Djatmiko Ichsani, Prabowo and Sutardi

---------- REVIEW ----------
This paper format is in accordance with ICOME'S 2013 paper template

UNIVERSITAS KRISTEN PETRA

Ekadewi Handoyo <ekadewi@petra.ac.id>

Letter of Acceptance and Invitation Letter

1 message

icome@its.ac.id <icome@its.ac.id> Tue, Jul 16, 2013 at 12:38 AM
To: ekadewi@peter.petra.ac.id

Dear Author,
We herewith to send you the invitation letter and letter of acceptance of ICOME 2013 in the attached files. Also we send you the conference's time schedule. If you want to know how to go to the conference venue please find in http://lombok-network.com/LOP_arr_schedule.htm.
Please don't hesitate to contact us if you have any further questions

Best Regards
ICOME COMMITTEE

Institut Teknologi Sepuluh Nopember (ITS)
http://www.its.ac.id

2 attachments

69.1.pdf
225K

SCHEDULE.pdf
158K